8. Abassi Z, Kotob S, Pieruzzi F, Abouassali M, Keiser HR, Fratantoni JC, Alayash AI. Effects of polymerization on the hypertensive action of diaspirin cross-linked hemoglobin in rats. J Lab Clin Med 1997;129:603–610.
9. Gould SA, Moore EE, Moore FA, Haenel JB, Burch JM, Sehgal H, Sehgal L, DeWoskin R, Moss GS. Clinical utility of human polymerized hemoglobin as a blood substitute after acute trauma and urgent surgery. J Trauma 1997;43:325–332.
10. Guyton AC, Ross JM, Carrier O, Walker JR. Evidence for tissue oxygen demand as the major factor causing autoregulation. Circ Res 1964;14:1–60.
11. Tsai AG, Kerger H, Intaglietta M. Microcirculatory consequences of blood substitution with αα-hemoglobin. In: Winslow RM, Vandegriff KD, Intaglietta M, editors. Blood substitutes: physiological basis of efficiency. Boston, MA: Birkhäuser; 1995. p 155–174.
12. Rohlfs RJ, Bruner E, Chiu A, Gonzales ML, Magde D. Arterial blood pressure responses to cell-free hemoglobin solutions and the reaction with nitric oxide. J Biol Chem 1998;273:12128–12134.
13. Winslow RM. αα-Crosslinked hemoglobin: was failure predicted by preclinical testing? Vox Sang 2000;79:1–20.
14. Komatsu T, Hamamatsu K, Wu J, Tsuchida E. Physicochemical properties and O_2-coordination structure of human serum albumin incorporating tetrakis(*o*-pivamido)phenylporphyrinatoiron(II) derivatives. Bioconjug Chem 1999;10:82–86.
15. Tsuchida E, Komatsu T, Matsukawa Y, Hamamatsu K, Wu J. Human serum albumin incorporating tetrakis(*o*-pivalamido)-phenylporphinatoiron(II) derivative as a totally synthetic O_2-carrying hemoprotein. Bioconjug Chem 1999;10:797–802.
16. Komatsu T, Matsukawa Y, Tsuchida E. Kinetics of CO- and O_2-binding to human serum albumin-heme hybrid. Bioconjug Chem 2000;11:772–776.
17. Komatsu T, Matsukawa Y, Tsuchida E. Reaction of nitric oxide with synthetic hemoprotein, human serum albumin incorporating tetraphenylporphinatoiron(II) derivatives. Bioconjug Chem 2001;12:71–75.
18. Tsuchida E, Komatsu T, Matsukawa Y, Nakagawa A, Sakai H, Kobayashi K, Suematsu M. Human serum albumin incorporating synthetic heme: red blood cell substitute without hypertension by nitric oxide scavenging. J Biomed Mater Res 2003; 64A:257–261.
19. Huang Y, Komatsu T, Nakagawa A, Tsuchida E, Kobayashi S. Compatibility *in vitro* of albumin-heme (O_2 carrier) with blood cell components. J Biomed Mater Res 2003;66A:292–297.
20. Komatsu T, Matsukawa Y, Tsuchida E. Effect of heme structure on O_2-binding properties of human serum albumin-heme hybrids: intramolecular histidine coordination provides a stable O_2-adduct complex. Bioconjug Chem 2002;13:397–402.
21. Tsuchida E, Komatsu T, Hamamatsu K, Matsukawa Y, Tajima A, Yoshizu A, Izumi Y, Kobayashi K. Exchange transfusion of albumin-heme as an artificial O_2-infusion into anesthetized rats: physiological responses, O_2-delivery and reduction of the oxidized hemin sites by red blood cells. Bioconjug Chem 2000; 11:46–50.
22. McCarthy MR, Vandegriff KD, Winslow RM. The role of facilitated diffusion in oxygen transport by cell-free hemoglobin: implication for the design of hemoglobin-based oxygen carriers. Biophys Chem 2001;92:103–117.
23. Vandegriff KD, Malavalli A, Wooldbridge J, Lohman J, Winslow RM. MP4, a new nonvasoactive PEG-Hb conjugate. Transfusion 2003;43:509–516.
24. Doherty DH, Doyle MP, Curry SR, Vali RJ, Fattor TJ, Olson JS, Lemon DD. Rate of reaction with nitric oxide determines the hypertensive effect of cell-free hemoglobin. Nat Biotechnol 1998;16:672–676.
25. Malek AM, Izumo S. Control of endothelial cell gene expression by flow. J Biomech 1995;28:1515–1528.
26. Tsai AG, Friesenecker B, McCarthy M, Sakai H, Intaglietta M. Plasma viscosity regulates capillary perfusion during extreme hemodilution in hamster skinfold model. Am J Physiol 1998: 275;H2170–H2180.

Available online at www.sciencedirect.com

SCIENCE DIRECT

Biochimica et Biophysica Acta 1675 (2004) 21–31

BIOCHIMICA ET BIOPHYSICA ACTA BBA

http://www.elsevier.com/locate/bba

Physicochemical characterization of cross-linked human serum albumin dimer and its synthetic heme hybrid as an oxygen carrier

Teruyuki Komatsu[a], Yukiko Oguro[a], Yuji Teramura[a], Shinji Takeoka[a], Junpei Okai[b], Makoto Anraku[b], Masaki Otagiri[b], Eishun Tsuchida[a,*]

[a]*Advanced Research Institute for Science and Engineering, Waseda University, 3-4-1 Okubo, Shinjuku-ku, Tokyo 169-8555, Japan*
[b]*Department of Pharmaceutics, Faculty of Pharmaceutical Sciences, Kumamoto University, 5-1 Oe-honmachi, Kumamoto 862-0973, Japan*

Received 13 May 2004; received in revised form 9 August 2004; accepted 10 August 2004
Available online 11 September 2004

Abstract

The recombinant human serum albumin (rHSA) dimer, which was cross-linked by a thiol group of Cys-34 with 1,6-bis(maleimido)hexane, has been physicochemically characterized. Reduction of the inert mixed-disulfide of Cys-34 beforehand improved the efficiency of the cross-linking reaction. The purified dimer showed a double mass and absorption coefficient, but unaltered molar ellipticity, isoelectric point (p*I*: 4.8) and denaturing temperature (65 °C). The concentration dependence of the colloid osmotic pressure (COP) demonstrated that the 8.5 g dL^{-1} dimer solution has the same COP with the physiological 5 g dL^{-1} rHSA. The antigenic epitopes of the albumin units are preserved after bridging the Cys-34, and the circulation lifetime of the ^{125}I-labeled variant in rat was 18 h. A total of 16 molecules of the tetrakis{(1-methylcyclohexanamido)phenyl}porphinatoiron(II) derivative (FecycP) is incorporated into the hydrophobic cavities of the HSA dimer, giving an albumin–heme hybrid in dimeric form. It can reversibly bind and release O_2 under physiological conditions (37 °C, pH 7.3) like hemoglobin or myoglobin. Magnetic circular dichroism (CD) revealed the formation of an O_2–adduct complex and laser flash photolysis experiments showed the three-component kinetics of the O_2-recombination reaction. The O_2-binding affinity and the O_2-association and -dissociation rate constants of this synthetic hemoprotein have also been evaluated.

Keywords: Human serum albumin dimer; Cross-linking; Colloid osmotic pressure; Synthetic heme; Albumin–heme dimer; Oxygen carrier

1. Introduction

Human serum albumin (HSA) is the most abundant plasma protein and contains 35 cysteines, of which 17 couples form intramolecular disulfide bonds to fold a single polypeptide as a unique heart-shape structure [1–4]. Only the first thiol residue in the chain, namely Cys-34, does not participate in the S–S bonding and functions as a binding site for the SH-involving ligands (cysteine, glutathione, and captopril), as well as for the various metal ions and nitric oxide [1,5]. Interestingly, two albumin molecules can associate to produce a dimer through an intermolecular disulfide bridge of Cys-34; approximately 5% of HSA is actually in a dimeric form in our bloodstream [6]. Hughes [7] initially prepared the HSA dimer by the addition of bifunctional $HgCl_2$, which causes Cys-34 to connect through mercury. Subsequent oxidation of this mercury dimer by treatment with iodine gave a disulfide-linked HSA [8]. It can also be directly prepared by oxidation of HSA with ferricyanide [9]. However, electron spin resonance measurements of HSA and the latest crystal structural analysis of the recombinant HSA (rHSA) revealed that Cys-34 locates in a hydrophobic crevice at a depth of 9.5 Å from the surface [2–4,10]. This implies that the intermolecular Cys-34 disulfide bridging might lead to flattening of the pocket. We have linked two rHSA molecules with a flexible bola-shape spacer, 1,6-bis(maleimido)hexane (BMH), which is long (16 Å) enough to connect the Cys-34 residues, to produce a new type of rHSA dimer (Fig. 1) [11].

* Corresponding author. Tel.: +81 3 5286 3120; fax: +81 3 3205 4740.
E-mail address: eishun@waseda.jp (E. Tsuchida).

0304-4165/$ - see front matter © 2004 Elsevier B.V. All rights reserved.
doi:10.1016/j.bbagen.2004.08.010

(A)

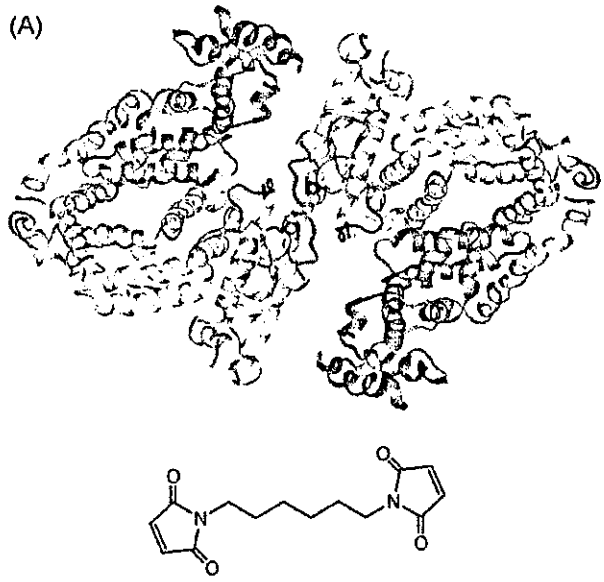

1,6-Bis(maleimido)hexane (BMH)

(B)

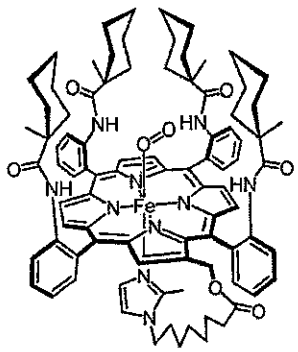

FecycP

Fig. 1. (A) Simulated structure of rHSA dimer cross-linked by Cys-34 with 1,6-bis(maleimido)hexane (BMH). The domains I, II, and III of each rHSA unit are colored white, yellow, and pink, respectively. The cross-linking agent (BMH) is shown in a space-filling representation and colored by atom type (carbon: green, nitrogen: blue, oxygen: red). The figure was made with insight II (Molecular Simulations) on the basis of the 1e78 available at the Brookhaven PDB. (B) Formula of synthetic heme, FecycP.

On the other hand, a maximum of eight molecules of synthetic heme with a covalently bound proximal base is incorporated into the hydrophobic cavities of rHSA, giving an albumin–heme hybrid, which can reversibly bind and release O_2 under physiological conditions (pH 7.3, 37 °C) like hemoglobin (Hb) or myoglobin (Mb) [12]. We have shown that this O_2-carrying plasma protein acts as a red blood cell (RBC) substitute in vitro and in vivo [13]. The only fault of this system is its relatively low heme concentration, which reflects the O_2 solubility in the medium. For instance, the albumin–heme solution with a physiological HSA concentration (≈0.75 mM) involves 6 mM of heme, which corresponds to only 65% of the amount in human blood ([heme]=9.2 mM). A highly condensed solution can dissolve more heme, however, the colloid osmotic pressure (COP) increases in proportion to the albumin concentration. We have found that a total of 16 molecules of 2-[8-{*N*-(2-methylimidazolyl)}octanoyloxymethyl]-5,10,15,20-tetrakis{α,α,α,α-*o*-(pivalamido)phenyl}porphinatoiron(II) (FepivP) was incorporated into the BMH-bridged HSA dimer, and this solution with 0.75 mM HSA includes 12 mM of heme [11]. The tertiary structures of the two protein-units might be intact after the cross-linking, and the ligand-binding capacity of the dimer became twofold in excess relative to that of the monomer. Consequently, the saline solution of the albumin–heme dimer can transport a large volume of O_2 in comparison to the human blood while maintaining its COP on a physiological level. A long persistence in circulation due to the large molecular size is also expected. In this paper, we report the efficient synthesis, physicochemical characterization, and preliminary pharmacokinetics of the BMH-bridged rHSA dimer. Furthermore, the O_2-binding properties of the albumin-heme dimer incorporating the FepivP analogue, 2-[8-{*N*-(2-methylimidazolyl)}octanoyloxymethyl]-5,10,15,20-tetrakis{α,α,α,α-*o*-(1-methylcyclohexanamido)phenyl}porphinatoiron(II) (FecycP, Fig. 1), are evaluated by magnetic circular dichroism and laser flash photolysis.

2. Material and methods

2.1. Materials

An rHSA (Albrec®, 25 wt.%) was provided from the NIPRO (Osaka). Ethanol, dithiothreitol (DTT), 2,2′ -dithiopyridine, and warfarin (all high-purity grades) were purchased from Kanto Chemical, (Tokyo) and used without further purification. 1,6-Bis(maleimido)hexane was purchased from Pierce Biotechnology (Rockford, USA). Diazepam was purchased from Wako Pure Chemical Ind., (Tokyo). 2-[8-{*N*-(2-Methylimidazolyl)}octanoyloxymethyl]-5,10,15,20-tetrakis{α,α,α,α-*o*-(1-methylcyclohexanamido)phenyl}porphinatoiron(II) (FecycP) was prepared according to our previously reported procedure [14].

2.2. Synthesis of rHSA dimer

Aqueous DTT (1.0 M, 0.24 mL) was added to the phosphate buffer solution (pH 7.0, 10 mM) of rHSA (0.75 mM, 80 mL) under nitrogen, and the solution was quickly mixed by a vortex mixer, followed by an incubation for 30 min at room temperature. The obtained rHSA in reduced form was washed with a total of 880-mL phosphate buffer (pH 7.0, 2.25 mM) using an ADVANTEC UHP-76K ultrafiltration system with a Q0500 076E membrane (cutoff Mw 50 kDa) and finally condensed to 26.7 mL ([rHSA]=2.25 mM). The mercapto-ratio of the Cys-34

was confirmed by the reaction with 2,2′ -ditiopyridine (2,2′ -DTP), which immediately coupled with the free thiol group to give 2-thiopyridinone (2-TP) with an absorption at 343 nm [molar absorption coefficient (ε_{343}): 8.1×10^3 M^{-1} cm^{-1}]. Quantitative assay of the produced 2-TP showed that the mercapto-ratio of Cys-34 was 100%. Ethanolic BMH (6.38 mM, 4.76 mL) divided into three portions was then slowly added dropwise into the rHSA solution within 1 h under an N_2 atmosphere, and gently stirred overnight at room temperature. The reaction kinetics was observed by the HPLC measurements. The HPLC system consisted of a Shimadzu LC-8A pump and a Shimadzu SPD-10A UV detector. A Shodex Protein KW-803 column was used and the mobile phase was phosphate buffered saline (PBS, pH 7.4) at 25 °C (1.0 mL min^{-1}). The dimer was purified by gel column chromatography with Sephacryl S-200 HR (Pharmacia, 5 cmϕ×40 cm) and PBS (pH 7.4) as the eluant (5.0 mL min^{-1}). These separations were performed using a BIO-RAD EGP Combo Rec system. The elution was monitored by absorption at 280 nm. The purity of the dimer was measured by the HPLC technique described above. The albumin concentrations were assayed by general bromcresol green (BCG) methods using a Wako AlbuminB-Test [15].

2.3. Physicochemical properties

The UV–Vis absorption spectra were recorded on a JASCO V-570 spectrophotometer. The measurements were normally carried out at 25 °C. Circular dichroism (CD) spectra were obtained using a JASCO J-725 spectropolarimeter. The rHSA samples' concentration was 2 μM in PBS, and quartz cuvettes with a 1-mm thickness were used for the measurements over the range of 195–250 nm. The matrix associated laser desorption ionization time-of-flight mass spectra (MALDI-TOF MS) were obtained using a Shimadzu AXIMA-CFR Kompact MALDI, which was calibrated by BSA (Sigma A-0281) and HSA (Sigma A-3782). The specimens were prepared by mixing the aqueous sample solution (10 μM, 1 μL) and matrix (10 mg mL^{-1} sinapinic acid in 40% aqueous CH_3CN, 1 μL) on the measuring plate and drying in air. The viscosity and density of the rHSA solutions (PBS, pH 7.4) were obtained using an Anton PAAR DSC 300 capillary viscometer at 37 °C. The isoelectric points and molecular weights were obtained by a Pharmacia Phastsystem using isoelectric focusing (IEF) in Phast Gel IEF 3-9 and Native-PAGE in Phast Gel Gradient 8–25, respectively. The colloid osmotic pressures of the rHSA solutions (PBS, pH 7.4) were measured by a WESCOR 4420 Colloid Osmometer at 25 °C. A membrane filter with a 30-kDa cutoff was used. Differential scanning calorimetry (DSC) was measured on a SEIKO Instruments DCS120 differential scanning calorimeter at the scan rate of 1 °C min^{-1} in the temperature range between 10 and 95 °C. The concentrations of the rHSA samples were 75 μM in PBS (pH 7.4).

2.4. Ligand binding constants

The PBS solution of ligand (warfarin or diazepam, 20 μM, 2 mL) was mixed with the rHSA sample in PBS (20 μM, 2 mL), and the unbound ligand fractions were separated by centrifugation (2000 rpm, 25 °C, 20 min) using a Millipore Centriplus YM-50. Adsorption of the ligand molecules onto the filtration membranes was negligible. The unbound ligand concentrations were determined by UV–Vis spectroscopic measurements.

2.5. Compatibility with blood components in vitro

Fresh whole blood was obtained from Wistar rats (300 g, male, Saitama Experimental Animals Supply, Japan) and stored in heparinized glass tubes. The rHSA samples (PBS, pH 7.4) were then slowly added to the blood at 50 vol.% concentrations (whole volume 2 mL). After 30 min, 30 μL of the sample was mixed with 100 μL of a Terumo ACD-A solution, which was diluted in advance with pure water by 1:10 (v/v). The blood cell numbers of the obtained samples were counted using a Sysmex KX-21 blood cell counting device. Furthermore, one drop of the incubated sample of the blood with the rHSA dimer was microscopically observed using an Olympus IX50 microscope with an IX70 CCD camera.

2.6. Immunogenicity

The Tris–HCl buffer solutions (TBS, pH 7.4, 50 mM, 50 μL) of the rHSA samples (10 μg mL^{-1}) were injected into a Nunc immunoplate and incubated at 4 °C overnight. The rHSA solutions in the wells were washed with TBS, and 2% skimmed milk was added to avoid the nonspecific binding of the antibody. After washing with TBS including 0.1% Tween 20 (Tween 20–TBS), anti-HSA polyclonal antibody (50 μL per well) was added and incubated for 2 h at 25 °C. The antibody was removed by aspiration, and 50 μL of horseradish peroxidase-labelled rabbit anti-IgG polyclonal antibody diluted 1/5000 by Tween 20–TBS was injected, following an incubation for 1 h at 25 °C. Finally, 100 μL of *o*-phenylenediamine substrate solution (400 mg mL^{-1} in 0.15 M citrate-phosphate buffer (pH 5.0) involving 0.1% H_2O_2) was put into each well. H_2SO_4 (2 M; 50 μL) was then added to stop the reaction. The resulting absorbance in each well was measured at 490 nm using a Japan InterMed Imunomini NJ-2300.

2.7. Circulation lifetime in vivo

The 125-Iodinated rHSA monomer and dimer were prepared by our previously reported procedures, and purified using a Pharmacia Bio-Gel PD-10 column [16]. The recovered ^{125}I-albumin had a specific activity of 2.0×10^7 cpm μg^{-1}, and was diluted by non-labeled albumin before intracardial administration into anesthetized Wistar rats

(200–210 g, male). The kinetics of the albumin clearance from the circulation was monitored by measuring the radioactivity in the plasma phase of blood taken from the lateral tail veins using an Aloka ARC 2000 Autowell Gamma Counter. Acid precipitability of the recovered radioactivity was also measured. The aqueous trichloroacetic acid (TCA, 25%, 0.1 mL) was first added to the plasma (20 μL) diluted with 5 g dL^{-1} rHSA (80 μL), followed by centrifugation (3000 rpm, 10 min). The precipitate was then washed with 12.5% TCA (0.2 mL) and the radioactivity of the pellet was measured. The rats were sacrificed at the end of the experiments by hemorrhage. The radioactivity of the excised organs was also measured as well. The care and handling of the animals were in accordance with NIH guidelines.

2.8. Preparation of albumin–heme dimer

The preparation of rHSA–FecycP dimer was carried out by mixing the EtOH solution of carbonyl-FecycP and an aqueous phosphate buffer solution of rHSA according to our previously reported procedures ([FecycP]/[rHSA]=16:1 (mol/mol)) [13]. The albumin concentrations were assayed by the general BCG methods described above, and the amount of FecycP was determined by the assay of the iron ion concentration using inductively coupled plasma spectrometry (ICP) with a Seiko Instruments SPS 7000A spectrometer.

2.9. Magnetic circular dichroism (MCD)

MCD spectra for the phosphate buffer solution of the rHSA–FecycP dimer (10 μM) under N_2, CO, and O_2 atmospheres were measured using a JASCO J-820 circular dichrometer fitted with a 1.5-T electromagnet. The accumulation times were normally three, and from each data point was subtracted the spectra without an electromagnetic (at 0 T) as the baseline.

2.10. O_2-Binding equilibrium and kinetics

O_2-Binding to FecycP was expressed by Eq. (1).

$$\text{FecycP} + O_2 \underset{k_{off}}{\overset{k_{on}}{\rightleftharpoons}} \text{FecycP}(O_2) \quad (K = k_{on}/k_{off}) \tag{1}$$

The O_2-binding affinity (gaseous pressure at half O_2-binding for heme, $P_{1/2}=1/K$) was determined by spectral changes at various partial pressure of O_2 as in previous reports [12,a,d,14]. The FecycP concentrations of 20 μM were normally used for the UV–Vis absorption spectroscopy. The spectra were recorded within the range of 350–700 nm. The half lifetime of the dioxygenated species of the rHSA–FecycP dimer was determined by the time dependence of the absorption intensity at 549 nm, which is based on the O_2–adduct complex. The association and dissociation rate constants for O_2 (k_{on}, k_{off}) were measured by a competitive rebinding technique using a Unisoku TSP-600 laser flash photolysis apparatus [12,17–19]. The absorption decays accompanying the O_2 association to the rHSA–FecycP dimer obeyed three-component kinetics. We employed triple-exponentials to analyze the absorption decays; $\Delta A(t)$ [12,a,b,],

$$\Delta A(t) = C_1\exp(-k_1 t) + C_2\exp(-k_2 t) + C_3\exp(-k_3 t) \tag{2}$$

where k_1, k_2, k_3 are apparent rate constants for the each reaction. The data were fit to this equation using a Solver in Excel 2003.

3. Results and discussion

3.1. Synthesis of rHSA dimer

In the neutral pH range (5.0–7.0), DTT selectively reduces the mixed-disulfide of Cys-34 in HSA or BSA [20–22]. In fact, the addition of the small molar excess DTT into the rHSA solution (phosphate buffer, pH 7.0, 10 mM) under an N_2 atmosphere led to complete reduction of Cys-34 (mercapto-ratio became 100%). After removing DTT, ethanolic BMH was dropwise added to the reduced rHSA to initiate the cross-linking reaction. The pretreatment with DTT significantly increased the yield of the dimer, and the rHSA concentration of 15 g dL^{-1} gave the highest yield of 45%, which is significantly improved from our previous result (Fig. 2) [11]. Several attempts to facilitate the dimerization

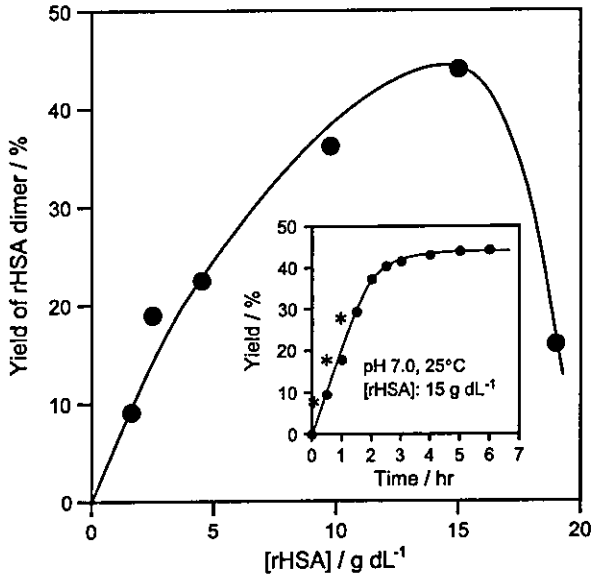

Fig. 2. The relationship between the rHSA concentration and yield of the rHSA dimer. The yields were determined based on the peak area in the HPLC elution curves. Inset shows the time course of the dimerization yield when the rHSA concentration was set at 15 g dL^{-1}. The asterisks indicate the time points when the EtOH solution of BMH was dropwise added. The total EtOH content in the reaction mixture was 15 vol.%.

unfortunately failed: (i) gentle heating (25–50 °C), (ii) changing the co-solvent from EtOH to DMF for dissolving the BMH, and molar ratio [BMH]/[rHSA]: 0.5–1.5, (iii) increasing the concentrations of co-solvents (<30%), and (iv) the further addition of the reactive rHSA monomer.

The HPLC elution curve of the reactant demonstrated only two peaks (rHSA monomer and dimer), which means that the bifunctional BMH was successfully bound to Cys-34 which led to dimer formation and not polymerization (Fig. 3). The yield reached a peak within 4 h (Fig. 2 inset). The addition of EtOH to the mixture (40 vol.%) immediately formed a white precipitate; this is similar to the well-known Cohn's methods [1,23]. However, the precipitate still contained the monomer component. In contrast, separation using gel column chromatography with Sephacryl S-200 HR gave the dimer with 99% purity and 80% recovery. Native-PAGE showed a single band in the molecular weight range of 13 kDa (Fig. 3, above). We could not detect the free thiol in the isolated rHSA dimer (mercapto-ratio: 0%), which is now available in gram quantities. The appearance of the obtained dimer solution (in PBS, 20 g dL^{-1}) did not change over 1 year at room temperature and underwent no aggregation and precipitation.

3.2. Physicochemical properties

The matrix associated laser desorption ionization time-of-flight mass spectroscopy (MALDI-TOF MS) of the BMH-bridged rHSA dimer showed a distinct sharp signal at *m/z* 132,741.3, which is in good agreement with the calculated mass (Mw. 133,179.6); the difference was only 0.3% (Table 1). The magnitudes of its UV–Vis absorption (λ_{max}: 280 nm) significantly increased compared to that of

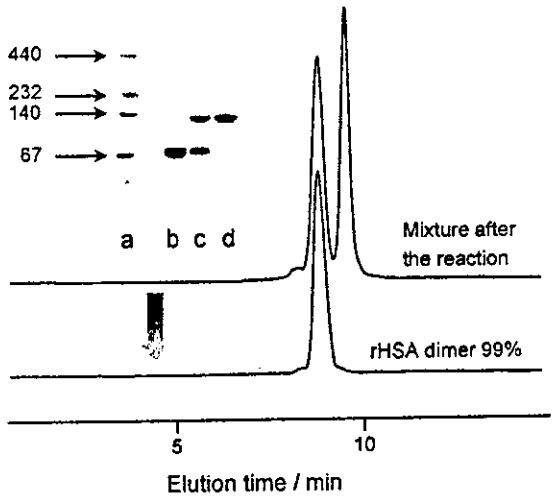

Fig. 3. HPLC elution curves of the rHSA dimer at 25 °C. The upper profile after the reaction indicated that the reactant consists of only the monomer and dimer. After gel column chromatography, the rHSA dimer was isolated with the purity of 99%. The left upper pattern is the native-PAGE electrophoresis of the rHSA dimer. a: markers, b: rHSA, c: mixture after the reaction, d: purified rHSA dimer.

Table 1
Physicochemical properties of rHSA dimer

	rHSA	rHSA dimer
Mw (Da)	66,331[a]	132,741[a]
	66×10^3 [b]	136×10^3 [b]
[calculated value]	66,451	133,180
Cys-34 mercapto ratio (%)	17	0
pI	4.8	4.8
ε_{280} (cm^{-1} M^{-1})	3.4×10^4	6.8×10^4
$[\theta]_{208}$ (deg cm^2 $dmol^{-1}$)	1.9×10^4	1.9×10^4
$[\theta]_{222}$ (deg cm^2 $dmol^{-1}$)	1.8×10^4	1.8×10^4

[a] Determined by MALDI-TOF/MS.
[b] Determined by [C] vs. COP/[C] (Fig. 5, inset).

rHSA with the same molar concentrations (Fig. 4(A)). The concentration of the albumin was carefully assayed by (i) BCG method [15] and (ii) weighing method with the weight of the freeze-dried sample and its molecular weight. While the molar absorption coefficient at 280 nm (ε_{280}: 6.8×10^4 M^{-1} cm^{-1}) became exactly twice the monomer's value (3.4×10^4 M^{-1} cm^{-1}), the CD spectral pattern (λ_{min}: 208, 222 nm) and the molar ellipticities at 208 and 222 nm ($[\theta]_{208}$: 1.9×10^4 deg cm^2 $dmol^{-1}$, $[\theta]_{222}$: 1.8×10^4 deg cm^2 $dmol^{-1}$) were identical to those of the monomer (Fig. 4(B), Table 1) [24,25]. It is appropriate to consider that the α-helix content of the each rHSA unit (67%) was unaltered [1–4]. The isoelectric point of the dimer (*pI*: 4.8) was also the same as that of rHSA. All these observations suggested that the secondary/tertiary structure and surface net charges of the rHSA units in the dimer did not change after the S–S disulfide bridging of Cys-34.

The DSC thermogram of this rHSA dimer showed an exothermic peak at 65 °C, which corresponds to its denaturing temperature (T_d). It has been shown that the T_d of HSA is largely dependent on the content of the

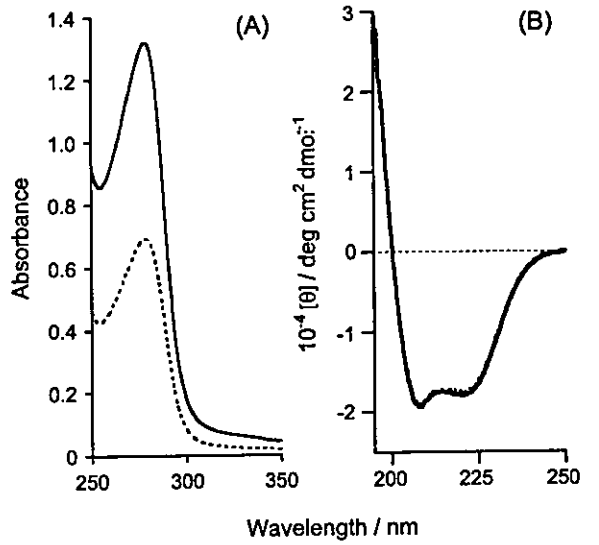

Fig. 4. (A) UV–Vis absorption spectra and (B) CD spectra of rHSA monomer (dotted line) and rHSA dimer (solid line) in PBS solution (pH 7.4) at 25 °C.

incorporated fatty acid, pH, and ionic strength [26,27]. In general, pasteurization for plasma HSA is performed at 60 °C for 10 h to eliminate the contaminations, e.g., hepatitis, HIV, and herpes virus [1]. Sodium caprylate and sodium *N*-acetyl-L-tryptophanate are commonly added to stabilize the albumin structure during the heat treatment [26]. Since the thermogram of the rHSA monomer under our sample conditions (PBS, pH 7.4) showed the T_d at 63 °C, we concluded that the rHSA dimer has the same thermodynamic stability with the monomer. Only the enthalpy change during the denaturation (ΔH) was slightly lower than the twice the monomer's value.

HSA acts as a carrier for many endogenous and exogenous substances in the blood circulation, and has two major specific drug binding sites, namely the warfarin site (Site I) and the indole and benzodiazepine site (Site II) [1,28]. We then determined the binding constants of typical ligands, warfarin (Site I-ligand) and diazepam (Site II-ligand), for the rHSA dimer using the ultracentrifugation method. In contrast to the results of the control experiments with rHSA, the amount of unbound ligand decreased to nearly half. The equilibria are expressed by following equations:

$$\mathrm{D} + \mathrm{L} \underset{}{\overset{K_1}{\rightleftharpoons}} \mathrm{D\text{-}L} \quad (3)$$

$$\mathrm{D\text{-}L} + \mathrm{L} \underset{}{\overset{K_2}{\rightleftharpoons}} \mathrm{D\text{-}L_2} \quad (4)$$

$$\mathrm{D} + 2\mathrm{L} \underset{}{\overset{K_1K_2}{\rightleftharpoons}} \mathrm{D\text{-}L_2} \quad (5)$$

where D is the rHSA dimer and L represents the ligand. The apparent binding constants (K_1K_2) of the warfarin and diazepam to the dimer were calculated to be 9.2×10^{10} and 3.0×10^{10} M^{-2}, respectively. If the each albumin unit independently accommodates one ligand, we estimated K_1 ($=K_2$) of each ligand as the square root of these values; 3.0×10^5 and 1.7×10^5 M^{-1}, respectively. They are almost in the same range as the binding constants for the monomeric rHSA (K_1), 3.8×10^5 and 1.4×10^5 M^{-1}, which means that neither the prevention nor the cooperation of the second ligand binding occurred in the dimer.

The attempt to prepare single crystals of the rHSA dimer for X-ray structural analysis failed, probably because it is likely to be very flexible at the BMH moiety. Transmission electron microscopy of the negatively stained samples showed homogeneous round particles with a diameter of 15–20 nm (not shown), however, the image is too small to obtain precise morphological information about the molecule.

The primary physiological function of HSA is the maintenance of COP within the blood vessels. Although HSA accounts for only 60% of the mass of the plasma protein, it contributes 80% of the COP. Two-thirds of this COP is simply the van't Hoff pressure and the other third arises from the Donnan effect of the negative charges of the plasma proteins, which is essentially due to albumin [1]. The relationship between the protein concentration and COP was observed for the rHSA and rHSA dimer solutions (Fig. 5). Both lines deviated upward from the linear correlation, because of the relatively larger value of the second virial coefficient, which is an index of the COP capacity, of the albumin molecule compared to those of the other plasma proteins. The measured rHSA monomer's curve coincided well to the previously reported result of Scatchard and co-workers (dotted line) [29]. The physiological concentration (5 g dL^{-1}) of rHSA represented the COP of 19 Torr. The careful inspections of their COP curves revealed that the 8.5 g dL^{-1} dimer solution has the same COP as the 5 g dL^{-1} rHSA. The plots of [C] versus COP/[C] gave a straight line, and the extrapolations to the y intercept afford the molecular weights of the monomer and dimer of 66×10^3 and 136×10^3 Da, respectively.

3.3. Viscosity and compatibility with blood components

Viscosity is a characteristic of proteins related to their size, shape, and conformation. The PBS solution of 8.5 g dL^{-1} rHSA dimer exhibited a Newtonian flow similar to the 5.0 g dL^{-1} rHSA, and showed a viscosity of 1.2 cP at a shear rate of 230 s^{-1} (Fig. 6). The dimer solution was then mixed with freshly drawn whole blood (1:1, v/v). The obtained suspension did not show any coagulation or precipitation for 6 h at 37 °C (after 6 h, hemolysis gradually took place even in the control experiment with saline or rHSA), and its viscosity profile was again Newtonian (1.8 cP at 230 s^{-1}). This result demonstrated good compatibility of the rHSA dimer with blood.

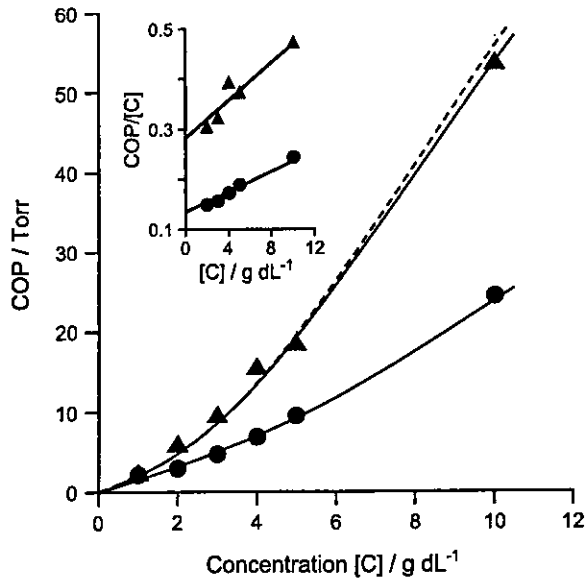

Fig. 5. Concentration [C] dependence of COP of rHSA monomer (▲) and rHSA dimer (●) in PBS (pH 7.4) at 22 °C. The dotted line represents the plasma HSA results taken from Ref. [29]. Inset shows relationship between [C] and COP/[C] for rHSA monomer (▲) and rHSA dimer (●).

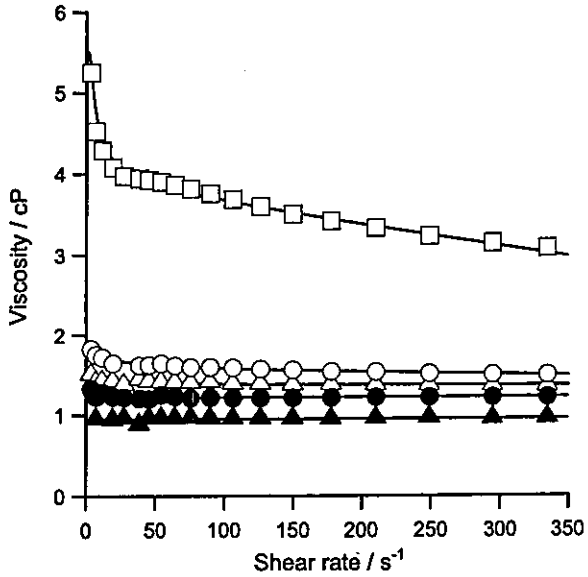

Fig. 6. Changes in the viscosity of rHSA monomer and rHSA dimer at various shear rates at 37 °C [□: whole blood, ●: 8.5 g dL^{-1} rHSA dimer, ▲: 5.0 g dL^{-1} rHSA, O: 8.5 g dL^{-1} rHSA dimer plus whole blood (1:1, v/v), △: 5.0 g dL^{-1} rHSA plus whole blood (1:1, v/v)].

In order to evaluate the blood compatibility of the 8.5 g dL^{-1} rHSA dimer solution in detail, the changes in the number of blood cell components [RBC, white blood cells (WBC), and platelets (PLT)] have been counted after the mixture (1:1, v/v). The numbers just after the addition of the rHSA dimer to the whole blood were reasonably reduced to half the basal values; the same behavior was observed in the control experiments with the saline or 5 g dL^{-1} rHSA [Fig. 7(A)]. Optical microscopic observations revealed that the homogeneous round shape of the RBCs was completely retained [Fig. 7(B)(C)]. Therefore, it can be considered that no specific interaction occurred between the rHSA dimer and the blood cell components in vitro.

3.4. Immunogenicity

We then analyzed the immunological reactivity of the rHSA dimer against the anti-HSA polyclonal antibody. The absorption intensity of the reactant plate with the dimer showed clear concentration dependence in the same manner as those of the rHSA and plasma HSA groups (Fig. 8). It is known that HSA has five major antigenic sites by analysis using synthetic peptides [30,31]. The sites are nearly α-helical regions in the HSA molecule and include charged and/or aromatic residues which are important for the presentation of antigenic determinations. We previously reported that the cross-reactivity of the anti-HSA polyclonal antibody to BSA was extremely low, despite their homologies of the sequences over 70% and its antigenic sites in the same regions [32]. The antigenic epitopes of rHSA are preserved after bridging the Cys-34.

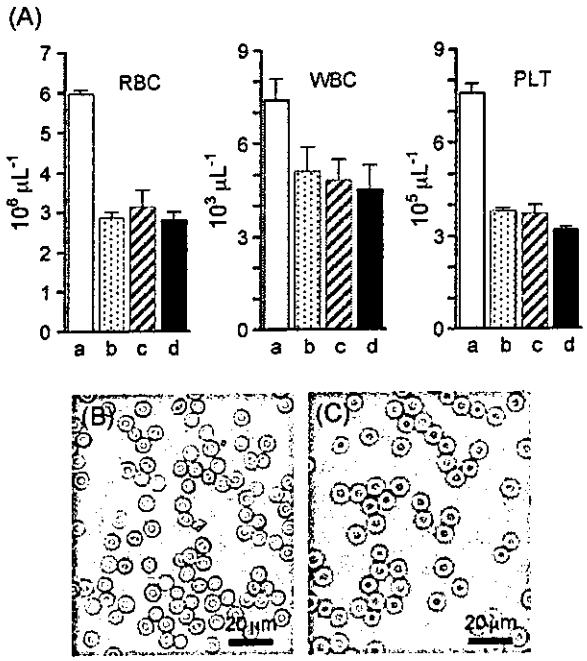

Fig. 7. (A) The blood cell (RBC, WRC, PLT) numbers in the blood suspension with the rHSA samples (1:1, v/v) at 25 °C [a: whole blood (basal value), b: with saline, c: with 5.0 g dL^{-1} rHSA, d: with 8.5 g dL^{-1} rHSA dimer]. Optical microscopic observations of (B) whole blood and (C) the blood suspension with the 8.5 g dL^{-1} rHSA dimer (1:1, v/v) (bar: 20 μm). The shape of the RBC with a diameter of ca. 8 μm did not change.

3.5. Circulation lifetime of ^{125}I-labeled rHSA dimer in rats

The rHSA and rHSA dimer labeled with ^{125}I were injected into rats to determine their blood circulation

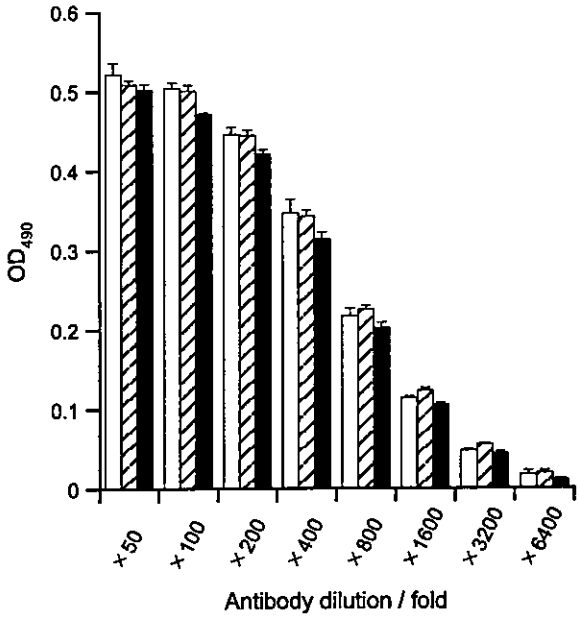

Fig. 8. Cross-reactivity of the anti-HSA polyclonal antibody with rHSA monomer and rHSA dimer [white bar: plasma HSA, diagonal bar: rHSA monomer, black bar: rHSA dimer]. All values are mean±S.D. (n=3).

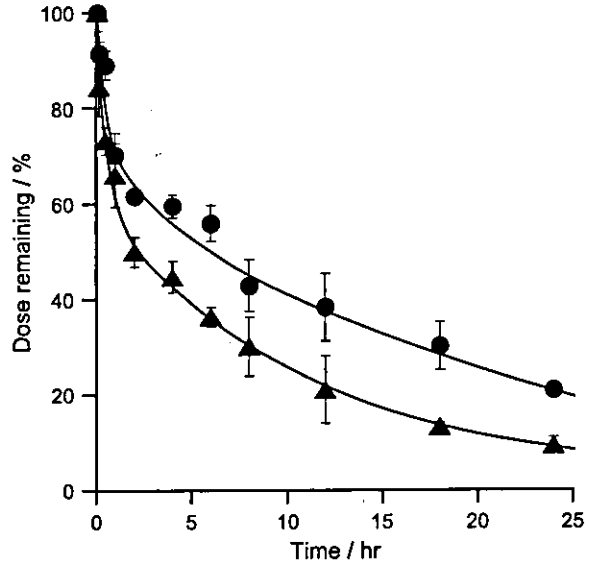

Fig. 9. Plasma levels of ^{125}I-rHSA monomer and dimer (1.0×10^7 cpm, 1.0 mg kg^{-1}) after intracardial administration into Wistar rats. All values are mean±S.D. (n=3).

lifetimes. The time courses of the radioactivity clearly showed two-phase kinetics, and significant differences between these two samples (Fig. 9). The half lifetimes ($\tau_{1/2}$) determined from the disappearance phase (β-phase) were 8.9 and 16.2 h for the monomer and dimer, respectively. The enlargement of the molecular size definitely led to retardation of extravasation through the vascular endothelium and produced a longer lifetime in the bloodstream. Radioactivity of the trichloroacetic acid precipitates recovered up to 95% the intensity, which means ^{125}I did not dissociate from the proteins. The tissue distributions of the rHSA dimer were in the skin, liver, kidney, and spleen (not shown), which took up most of the radioactivity, and we could not find any differences to that of the rHSA monomer.

More recently, McCurdy et al. [33] reported that a reiterated form of recombinant rabbit serum albumin (rRSA), in which two copies of the C34A rRSA mutant were joined with the C-terminus and N-terminus by a hexaglycine spacer, was more rapidly cleared ($\tau_{1/2}$: 3.0 days) in vivo (rabbit) than the corresponding monomer, C34A rRSA ($\tau_{1/2}$: 4.9 days). They postulated that the mechanism of this quick clearance of the dimer appears to involve the reticuloendothelial system (two binding sites on a dimer molecule to phagocytic cells may underlie the increased rate); and also suggested that the albumin dimerization through Cys-34 probably does not substantially contribute to the albumin metabolism. However, our results clearly showed that the Cys-34 BMH-bridged rHSA dimer has the longer circulation lifetime relative to that of the rHSA monomer. This opposite conclusion presumably arises from the differences in the chemical structure of the cross-linking agents, highly-ordered structure of the albumin dimer itself, and mammal species in the experimental protocol.

3.6. Albumin–heme dimer and its O_2-binding

Since a maximum of eight FecycPs (Fig. 1) was incorporated into certain domains of rHSA [12,d,], we postulated that the rHSA dimer can capture a twofold molar excess of FecycP molecules relative to the monomer. From the quantitative analyses of the amount of rHSA and FecycP in the hemoprotein, the ratio of the FecycP/rHSA (mol/mol) was determined to be 15.7 for the mixing ratio (m) of 16 and 16.4 for the m of 20. Thus, we concluded that the maximum binding numbers of FecycP to an rHSA dimer were 16, the same as FepivP [11]. The obtained red-solution of the rHSA–FecycP dimer was stored for more than 1 year at 4 °C without any aggregation and precipitation.

The UV–Vis absorption spectrum of the aqueous rHSA–FecycP dimer solution in an N_2 atmosphere showed the formation of a typical five-N-coordinate high-spin complex of porphyrinatoiron(II) (λ_{max}: 444, 539, 565 nm) [12,14,17,19]. Upon exposure of this solution to O_2, the absorption spectral pattern immediately changed to that of a dioxygenated species (λ_{max}: 426, 549 nm). This O_2-binding reaction was reversible and kinetically stable under physiological conditions (pH 7.3, 37 °C). After admitting the CO gas, the O_2–addcut complex moved to the very stable carbonyl low-spin complex (λ_{max}: 427, 539 nm) (Fig. 10).

We then employed MCD spectroscopy to characterize the coordination structure of the FecycP in the rHSA dimer. Under an N_2 atmosphere, the MCD showed a well-characterized spectrum of a mono-imidazole ligated five-

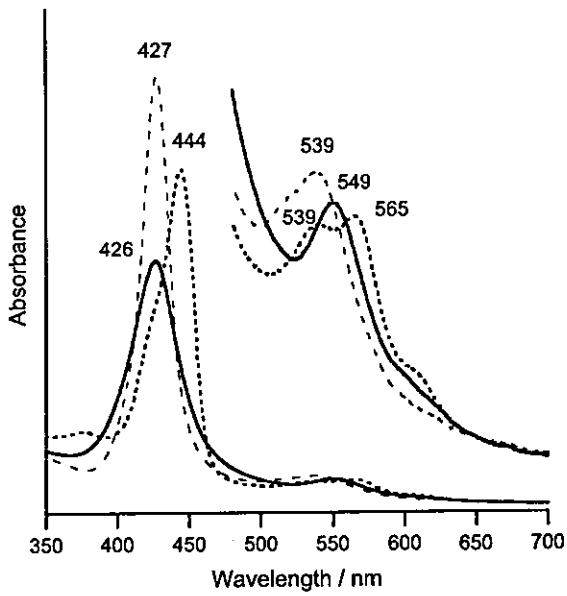

Fig. 10. UV–Vis absorption spectral changes of the rHSA–FecycP dimer in phosphate buffer solution (pH 7.3) at various conditions (25 °C) (dotted line: under N_2; solid line: under O_2; broken line: under CO).

coordinate high-spin porphyrinatoiron(II), which is in contrast to that of the six-coordinate low-spin state with the bis-imidazole ligated complex (Fig. 11) [34]. This observation indicates that no amino acid residue binds to the sixth position of FecycP in the rHSA structure under an N_2 atmosphere. The admission of O_2 gas yields an S-shaped A-term MCD in the Soret-band region, which shows the formation of an O_2–adduct complex as observed in the spectra of the other dioxygenated porphyrinatoiron(II) [34]. The CO adduct is also low spin and showed a similar A-term MCD band with a strong intensity. In all cases, the pattern in the Q-band regions coincided well with those reported previously [34].

The autooxidation reaction of the oxy state (λ_{max}: 549 nm) slowly occurred and the absorption intensity of 549 nm almost disappeared after 36 h, leading to the formation of the inactive Fe(III)cycP. The half-life of the dioxygenated species ($\tau_{1/2}$) was 6 h at 37 °C, which is significantly longer than that of our previous results for the rHSA–FepivP dimer ($\tau_{1/2}$: 2 h) [11]. The hydrophobic cyclohexanoyl fences on the porphyrin ring plane could effectively retard the autooxidation through the proton-driven process.

3.7. O_2-Binding kinetics and equilibrium of albumin–heme dimer

The association and dissociation rate constants for O_2 (k_{on}, k_{off}) were explored by laser flash photolysis. The absorption decays accompanying the O_2 recombination were composed of three-component kinetics, and the curves were fit by a triple-exponential equation [12,a,b,14]. The minor (less than 12%) component k_1, which is the fastest rate constant, is presumably correlated with a base

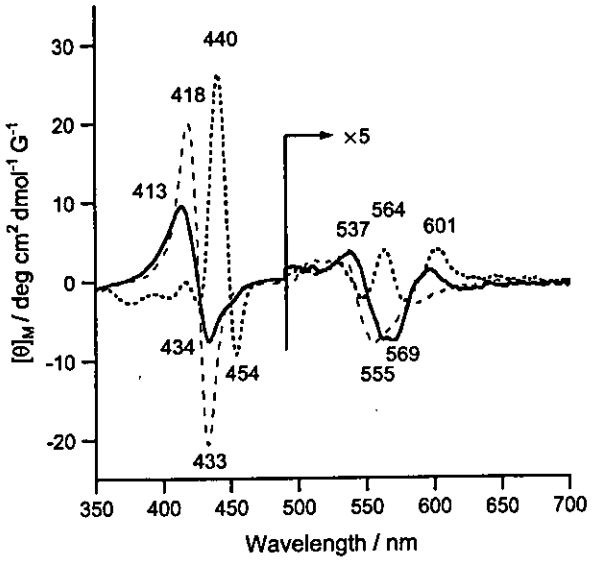

Fig. 11. MCD spectral changes of the rHSA–FecycP dimer in phosphate buffer solution (pH 7.3) at various conditions (25 °C) (dotted line: under N_2; solid line: under O_2; broken line: under CO).

Table 2
O_2-Binding parameters of the rHSA–FecycP dimer in phosphate buffer solution (pH 7.3) at 25 °C

	k_{on} (M^{-1} s^{-1})	k'_{on} (M^{-1} s^{-1})	k_{off} (s^{-1})	k'_{off} (s^{-1})	$P_{1/2}$ (Torr)[a]
rHSA–FecycP dimer	2.8×10^7	4.8×10^6	6.7×10^2	1.2×10^2	38
rHSA–FecycP	4.6×10^7	7.3×10^6	9.8×10^2	1.6×10^2	35
Hb (T-state)[b]	2.9×10^6		1.8×10^2		40

[a] At 37 °C. [b]pH 7.0, 20 °C, from Ref. [36].

elimination reaction [35]. From the slope of the linear plots of k_2 and k_3 versus the O_2 concentration, two association rate constants for the fast O_2 rebinding (k_{on}) and the slow O_2 rebinding were obtained (Table 2). The k_{on} values are 5.8-fold grater than k'_{on}, and the amplitude ratio of the fast and slow reactions was approximately 5/3. The O_2 association to FecycPs incorporated in the certain domains of the rHSA dimer is largely influenced by the protein environments surrounding each iron center of FecycP, for example, steric hindrance by the amino acid residues and/or difference in polarity. Six of the 16 sites of FecycP in the rHSA dimer are estimated to be the slow sites for the O_2 association.

The O_2-binding affinity ($P_{1/2}$) of the rHSA–FecycP dimer was determined to be 38 Torr at 37 °C on the basis of the UV–Vis spectral changes by O_2 titration [12,14,17–19]. The obtained $P_{1/2}$ is very close to that of rHSA–FecycP in the monomeric form and T-state Hb (Table 2) [12,d,35]. The O_2-dissociation rate constants were also calculated by k_{on}/K.

The rHSA–FecycP dimer did not show a cooperative O_2-binding profile like that seen in RBC; the Hill coefficient was 1.0 (Fig. 12). Although $P_{1/2}$ is slightly lower than that of RBC, the O_2-transporting efficiency (OTE) of the rHSA–FecycP dimer between the lungs (P_{O_2}: 110 Torr) and muscle

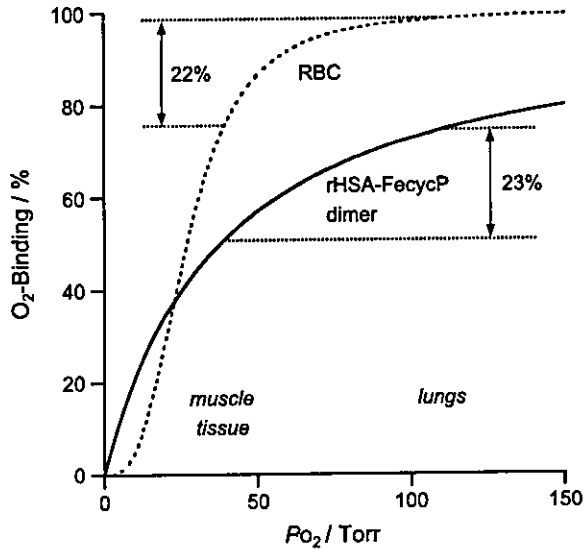

Fig. 12. OEC curve of the rHSA–FecycP dimer at 37 °C.

tissue (P_{O_2}: 40 Torr) (23%) becomes slightly higher than that of the human RBC (22%).

4. Conclusions

The obvious characteristics of the rHSA dimer cross-linked with the bola-shaped bismaleimide are as follows: (i) unaltered essential properties of the albumin units (the secondary/tertiary structure, surface net charges, thermostability), (ii) excess ligand-binding capacity relative to the monomer while maintaining its COP at the physiological value, (iii) good blood compatibility and identical antigenic epitopes with the monomer, and (iv) longer half-life in the bloodstream and similar tissue distributions with rHSA. Furthermore, (v) one molecule of the rHSA dimer incorporates 16 FecycPs, which is exactly twice the amount compared to that of the monomeric rHSA, and the obtained hemoprotein can reversibly bind and release O_2 under physiological conditions. (vi) The 8.5 g dL^{-1} rHSA–FecycP dimer solution satisfies the initial clinical requirements for the O_2-carrier as an RBC substitute, which transports 10 mM O_2 (compared to 9.2 mM in the human blood) while maintaining the COP at a constant 19 Torr.

Acknowledgements

This work was partially supported by Grant-in-Aid for Scientific Research (no. 16350093) from JSPS, and Grant-in-Aid for Exploratory Research (no. 16655049) from MEXT Japan, and Health Science Research Grants (Regulatory Science) from MHLW Japan.

References

[1] T. Peters Jr., All about Albumin. Biochemistry, Genetics, and Medical Applications, Academic Press, San Diego, 1996, and reference therein.
[2] D.C. Carter, J.X. Ho, Structure of serum albumin, Adv. Protein Chem. 45 (1994) 153–203.
[3] S. Curry, P. Brick, N.P. Franks, Fatty acid binding to human serum albumin: new insights from crystallographic studies, Biochim. Biophys. Acta 1441 (1999) 131–140.
[4] S. Sugio, A. Kashima, S. Mochizuki, M. Noda, K. Kobayashi, Crystal structure of human serum albumin at 2.5 Å resolution, Protein Eng. 12 (1999) 439–446.
[5] DJ. Meyer, H. Kramer, N. Özer, B. Coles, B. Ketterer, Kinetics and equiliburia of *S*-nitrosothiol–thiol exchange between glutathione, cysteine, penicillamines and serum-albumin, FEBS Lett. 345 (1994) 177–180.
[6] T. Peters Jr., Serum albumin, Adv. Protein Chem. 37 (1985) 161–245.
[7] a W.L. Hughes, The proteins of blood plasma, in: H. Neurath, K. Bailey (Eds.), The Proteins, vol. IIB, Academic Press, New York, 1954, pp. 663–734;
b W.L. Hughes, H.M. Dintzis, Crystallization of the mercury dimers of human and bovine mercaptalbumin, J. Biol. Chem. 239 (1964) 845–849.
[8] R. Straessle, A disulfide dimer of human mercaptalbumin, J. Am. Chem. Soc. 76 (1954) 3138–3142.
[9] L.-O. Anderson, Hydrolysis of disulfide bonds in weakly alkaline media II. Bovine serum albumin dimer, Biochim. Biophys. Acta 117 (1966) 115–133.
[10] C.N. Cornell, R. Chang, L.J. Kaplan, The environment of the sulfhydryl group in human plasma albumin as determined by spin labeling, Arch. Biochem. Biophys. 209 (1981) 1–6.
[11] T. Komatsu, K. Hamamatsu, E. Tsuchida, Cross-linked human serum albumin dimer incorporating sixteen (tetraphenylporphinato)iron(II) derivatives: synthesis, characterization, and O_2-binding property, Macromolecules 32 (1999) 8388–8391.
[12] (a) E. Tsuchida, T. Komatsu, Y. Matsukawa, K. Hamamatsu, J. Wu, Human serum albumin incorporating tetrakis(*o*-pivalamido)phenylporphinatoiron(II) derivative as a totally synthetic O_2-carrying hemoprotein, Bioconj. Chem. 10 (1999) 797–802;
(b) T. Komatsu, Y. Matsukawa, E. Tsuchida, Kinetics of CO and O_2 binding to human serum albumin–heme hybrid, Bioconj. Chem. 11 (2000) 772–776;
(c) T. Komatsu, Y. Matsukawa, E. Tsuchida, Reaction of nitric oxide with synthetic hemoprotein, human serum albumin incorporating tetraphenylporphinatoiron(II) derivatives, Bioconj. Chem. 12 (2001) 71–75;
(d) T. Komatsu, Y. Matsukawa, E. Tsuchida, Effect of heme structure on O_2-binding properties of human serum albumin–heme hybrids: intramolecular histidine coordination provides a stable O_2–adduct complex, Bioconj. Chem. 13 (2002) 397–402.
[13] (a) E. Tsuchida, T. Komatsu, K. Hamamatsu, Y. Matsukawa, A. Tajima, A. Yoshizu, Y. Izumi, K. Kobayashi, Exchange transfusion of albumin–heme as an artificial O_2-infusion into anesthetized rats: physiological responses, O_2-delivery and reduction of the oxidized hemin sites by red blood cells, Bioconj. Chem. 11 (2000) 46–50;
(b) Y. Huang, T. Komatsu, A. Nakagawa, E. Tsuchida, S. Kobayashi, Compatibility in vitro of albumin–heme (O_2-carrier) with blood cell components, J. Biomed. Mater. Res. 66A (2003) 292–297;
(c) E. Tsuchida, T. Komatsu, Y. Matsukawa, A. Nakagawa, H. Sakai, K. Kobayashi, M. Suematsu, Human serum albumin incorporating synthetic heme: red blood cell substitute without hypertension by nitric oxide scavenging, J. Biomed. Mater. Res. 64A (2003) 257–261.
[14] E. Tsuchida, T. Komatsu, K. Arai, H. Nishide, Synthesis and O_2-binding properties of tetraphenylporphyrinatoiron(II) derivatives bearing a proximal imidazole covalently bound at the β-pyrrolic position, J. Chem. Soc., Perkin Trans. 2 1995 (1995) 747–753.
[15] B.T. Doumas, W.A. Watson, H.G. Biggs, Albumin standards and measurement of serum albumin with bromcresol green, Clin. Chim. Acta 31 (1971) 87–96.
[16] H. Watanabe, K. Yamasaki, U. Kragh-Hansen, S. Tanase, K. Harada, A. Suenaga, M. Otagiri, In vivo and in vitro properties of recombinant human serum albumin from *Pichia pastoris* purified by a method of short processing time, Pharm. Res. 18 (2001) 1775–1781.
[17] J.P. Collman, J.I. Brauman, B.L. Iverson, J.L. Sessler, R.M. Morris, Q.H. Gibson, O_2 and CO Binding to iron(II) porphyrins: a comparison of the "picket fence" and "pocket" porphyrins, J. Am. Chem. Soc. 105 (1983) 3052–3064.
[18] T.G. Traylor, S. Tsuchiya, D. Campbell, M. Mitchell, D. Stynes, N. Koga, Anthracene heme cyclophanes: steric effects in CO, O_2, and RNC binding, J. Am. Chem. Soc. 107 (1985) 604–614.
[19] E. Tsuchida, T. Komatsu, K. Arai, H. Nishide, Synthesis and dioxygen-binding properties of double-sided porphyrinatoiron(II) complexes bearing covalently bound axial imidazole, J. Chem. Soc., Dalton Trans. 1993 (1993) 2465–2469.
[20] E. Katchalski, G.S. Benjamin, V. Gross, The availability of the disulfide bonds of human and bovine serum albumin and of bovine g-globulin to reduction by thioglycolic acid, J. Am. Chem. Soc. 79 (1957) 4096–4099.

[21] D.R. Grassetti, J.F. Murray Jr., Determination of sulfhydryl groups with 2,2' - or 4,4' -dithiopyridine, Arch. Biochem. Biophys. 119 (1967) 41–49.
[22] A.O. Pedersen, J. Jacobsen, Reactivity of the thiol group in human and bovine albumin at pH 3–9, as measured by exchange with 2,2' - dithiodipyridine, Eur. J. Biochem. 106 (1980) 291–295.
[23] E.J. Cohn, The properties and functions of the plasma proteins, with a consideration of the methods for their separation and purification, Chem. Rev. 28 (1941) 395–417.
[24] I. Sjöholm, I. Ljungstedt, Studies on the tryptophan and drug-binding properties of human serum albumin fragments by affinity chromatography and circular dichroism measurements, J. Biol. Chem. 248 (1973) 8434–8441.
[25] A. Sumi, W. Ohtani, K. Kobayashi, T. Ohmura, K. Yokoyama, N. Nishida, T. Suyama, Purification and physicochemical properties of recombinant human serum albumin, in: C. Rivat, J.-F. Stoltz (Eds.), Biotechnology of Blood Proteins, vol. 227, John Libbey Eurotext, Montrouge, 1993, pp. 293–298.
[26] S. Gumpen, P.O. Hegg, H. Martens, Thermal stability of fatty acid–serum albumin complexes studies by differential scanning calorimetry, Biochim. Biophys. Acta 574 (1979) 189–196.
[27] T. Kosa, M. Maruyama, M. Otagiri, Species differences of serum albumins: II. Chemical and thermal stability, Pharm. Res. 15 (1998) 449–454.
[28] a G. Sudlow, D.J. Birkett, D.N. Wade, The Characterization of two specific drug binding sites on human serum albumin, Mol. Pharmacol. 11 (1975) 824–832;
b G. Sudlow, D.J. Birkett, D.N. Wade, Further characterization of specific drug binding sites on human serum albumin, Mol. Pharmacol. 12 (1976) 1052–1061.
[29] G. Scatchard, A.C. Batchelder, A. Brown, Chemical, clinical, and immunological studies on the products of human plasma fractionation: VI. The osmotic pressure of plasma and of serum albumin, J. Clin. Invest. 23 (1944) 165–170.
[30] S. Sakata, M.Z. Atassi, Immunochemistry of serum albumin. X. Five major antigenic sites of human serum albumin are extrapolated from bovine albumin and confirmed by synthetic peptides, Mol. Immunol. 17 (1980) 139–142.
[31] C. Lapresle, N. Doyen, Studies of an antigenic site of human-serum albumin with monoclonal-antibodies, Mol. Immunol. 20 (1983) 549–555.
[32] W. Ohtani, Y. Nawa, K. Takeshima, H. Kamuro, K. Kobayashi, T. Ohmura, Physicochemical and immunochemical properties of recombinant human serum albumin from *Pichia pastoris*, Anal. Biochem. 256 (1998) 56–62.
[33] T.R. McCurdy, S. Gataiance, L.J. Eltringham-Smith, WP. Sheffield, A covalently linked recombinant albumin dimer is more rapidly cleared in vivo than are wild-type and mutant C34A albumin, J. Lab. Clin. Med. 143 (2004) 115–124.
[34] a J.P. Collman, J.I. Brauman, K.M. Doxsee, T.R. Halbert, E. Bunnenberg, R.E. Linder, G.N. LaMar, J.D. Guadio, G. Lang, K. Spartalian, Synthesis and characterization of "tailed picket fence" porphyrins, J. Am. Chem. Soc. 102 (1980) 4182–4192;
b J.P. Collman, F. Basolo, E. Bunnenberg, T.C. Collins, J.H. Dawson, P.E. Ellis Jr., M.L. Marrocco, A. Moscowitz, J.L. Sessler, T. Szymanski, Use of magnetic circular dichroism to determine axial ligation for some sterically encumbered iron(II) porphyrin complexes, J. Am. Chem. Soc. 103 (1981) 5636–5648;
c J.P. Collman, J.I. Brauman, T.J. Collins, B.L. Iverson, G. Lang, R.B. Pettman, J.L. Sessler, M.A. Walters, Synthesis and characterization of the "pocket" porphyrins, J. Am. Chem. Soc. 105 (1983) 3038–3052.
[35] J. Geibel, J. Cannon, D. Campbell, T.G. Traylor, Model compounds for R-state and T-state hemoglobins, J. Am. Chem. Soc. 100 (1978) 3575–3585.
[36] C.A. Sawicki, Q.H. Gibson, Properties of the T state of human oxyhemoglobin studied by laser photolysis, J. Biol. Chem. Soc. 252 (1977) 7538–7547.

Biomaterials

Safety Evaluation of an Artificial O_2 Carrier as a Red Blood Cell Substitute by Blood Biochemical Tests and Histopathology Observations

YUBIN HUANG,* TERUYUKI KOMATSU,* HISASHI YAMAMOTO,† HIROHISA HORINOUCHI,‡ KOICHI KOBAYASHI,‡ AND EISHUN TSUCHIDA*

Recombinant human serum albumin (rHSA) incorporating synthetic heme with a covalently linked proximal base (albumin-heme [rHSA-heme]) is an artificial O_2 carrier that can transport O_2 like hemoglobin does in the blood stream. To evaluate the clinical safety of this compound, 20% and 40% exchange transfusions with rHSA-heme into anesthetized rats were followed by blood biochemical tests and histopathologic observations for 7 days. In the 20% rHSA-heme group, a total of 30 analytes by blood biochemical tests showed almost the same values as those observed in the reference 20% rHSA group. Although some abnormal values for liver parameters were found in the 40% rHSA-heme group, they returned to normal after 7 days. Histopathologic observations indicated that the administration of rHSA-heme in a volume of 20% total blood volume did not produce any negative side effects on the vital organs. *ASAIO Journal* 2004; 50:525–529.

Hemoglobin (Hb)-based O_2 carriers have been studied as red blood cell substitutes or as an O_2 therapeutic.[1–3] The advantages of these O_2 carriers are 1) the absence of a blood type antigen and infectious virus, 2) a small particle size for penetration through constricted vessels where red blood cells cannot penetrate, and 3) stability for long-term storage. The first generation products (Hemolink, Polyheme, and Hemopure),[4] which are currently in clinical testing, have been followed by second generation materials (Hemospan™ [MP4],[5] adenosine-GSH-Hb,[6] and SOD-catalase-Hb[7] under development. We have developed an entirely synthetic O_2 carrier without using Hb. Recombinant human serum albumin (rHSA) incorporates a synthetic heme (2-[8-{*N*-(2-methylimidazolyl)}octanoyloxymethyl]-5,10,15,20-tetrakis {α,α,α,α-*o*-(1-methylcyclohexanamido)}phenylporphinatoiron(II) (**Figure 1**), providing an artificial hemoprotein (albumin-heme [rHSA-heme]), which has the potential to bind and release O_2 under physiologic conditions (pH 7.3, 37°C) in the same manner as Hb.[8–12] Because the rHSA-heme molecule is totally synthetic, there is absolutely no concern for infection with pathogens and virus. The *in vitro* experiments have indicated that the rHSA-heme solutions have a high compatibility with blood cell components.[12] Furthermore, we found that vasoconstriction was not observed after administration of rHSA-heme into the circulatory system because of its low permeability through the vascular endothelium; rHSA-heme does not deplete nitric oxide (endothelium-derived relaxing factor).[13] Our recent study of a 30% exchange transfusion with rHSA-heme after 70% hemodilution with 5% (by weight) rHSA in anesthetized rats showed that injection of this material improved the circulatory blood volume and resuscitated the animals from shock.[14] To evaluate the clinical safety of this material as a red blood cell substitute, 20% and 40% exchange transfusions in anesthetized rats were studied using blood biochemical testing and histopathologic observations for 7 days.

Materials and Methods

Preparation of rHSA-Heme

The rHSA (Albrec, 25% by weight) was provided by the NIPRO Corp. (Osaka, Japan). The rHSA-heme solution (rHSA: 4.9% rHSA by weight, pH 7.45; heme: 2.8 mmol/L heme, colloid osmotic pressure (COP) 18 torr, osmolarity 300 mOsm, viscosity 1.1 cP, and endotoxin <0.1 EU/ml) was prepared according to our previously reported procedure.[10,14,15] The other physicochemical properties of rHSA-heme (molecular weight 72.3 kDa, O_2 binding affinity [$p_{1/2}O_2$] 37 torr, and isoelectric point 4.8) have been reported elsewhere.[10] The half-life of the oxygenated rHSA-heme against the ferric state was 9 hours at 37°C *in vitro*.[10]

Exchange Transfusion with rHSA-Heme in Anesthetized Rats

The investigations were carried out in 60 male Wister rats (312 ± 3.0 gm). The details of the experimental setup (anesthesia and catheterization) were the same as our former protocol reported elswhere.[14,15] The total blood volume of a rat was estimated to be 64 ml/kg body weight. The 20% exchange transfusion was achieved by four cycles of repeated blood withdrawal *via* the common carotid artery (1 ml, 1 ml/min) and the rHSA-heme infusion into the femoral vein (1 ml, 1 ml/min; 20% rHSA-heme group, n = 12). The 40% exchange transfu-

From the *Advanced Research Institute for Science and Engineering, Waseda University, Shinjuku-ku, Tokyo; the †Pharmaceutical Research Center, NIPRO Corp., Kusatsu-shi, Shiga; and the ‡Department of General Thoracic Surgery, School of Medicine, Keio University, Shinjuku-ku, Tokyo, Japan.

Submitted for consideration June 2004; accepted for publication in revised form August 2004.

This work was partially supported by a grant-in-aid for scientific research (No. 16350093) from JSPS, a grant-in-aid for exploratory research (No. 16655049) from MEXT Japan, and health science research grants (regulatory science) from MHLW Japan.

Address correspondence to: Eishun Tsuchida, Advanced Research Institute for Science and Engineering, Waseda University, 3-4-1 Okubo, Shinjuku-ku, Tokyo 169-8555, Japan.

DOI: 10.1097/01.MAT.0000144361.60280.DA

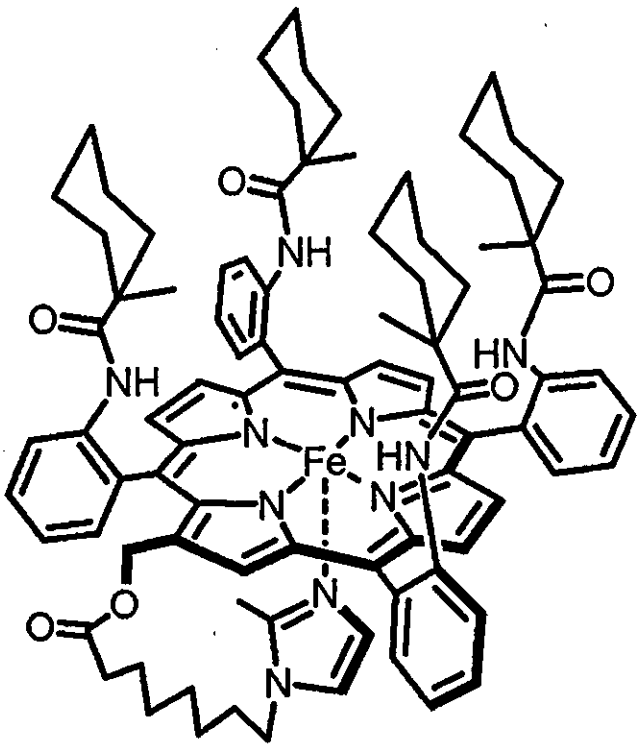

Figure 1. Chemical compound of entirely synthetic O_2 carrier without using Hb.

sion was performed by eight cycles of identical withdrawal/infusion (40% rHSA-heme group, n = 12). As a reference, a 5 gm/dl rHSA solution was given to other rats in the same ratios (20% rHSA group and 40% rHSA group, n = 12 each). Furthermore, 12 rats without blood exchange (anesthesia and surgery only) were also used as the control group. After the blood exchange transfusion, the animals were sutured and returned to their home cages. Their appearance and body weights were observed on days1, 3, and 7 after surgery.

After days 1 and 7, 4 ml of venous blood was taken from 6 rats in each group and centrifuged at 4°C (Beckman Coulter Co., Optima LE-80K for 3,500 rpm, 10 min). The plasma phase was frozen (−20°C) for the blood biochemical tests. The rats were sacrificed by venesection and the weights of the isolated liver, kidney, spleen, lung, and heart were measured. All animal handling and care were in accordance with NIH guidelines. The protocol details were approved by the Animal Care and Use Committee of Keio University.

Blood Biochemical Tests

A total of 30 analytes (total protein, albumin, albumin-globulin ratio, aspartate aminotransferase [AST], alanine aminotransferase [ALT], lactate dehydrogenase [LDH], alkaline phosphatase, γ-glutamyltransferase, leucine aminopeptidase [LAP], choline esterase, total bilirubin, direct bililubin, creatinine, blood urea nitrogen, uric acid, amylase, lipase, creatine phosphokinase, total cholesterol, free cholesterol, cholesterol ester [EChol], β-lipoprotein, high density lipoprotein [HDL] cholesterol, neutral fat [*i.e.*, triglyceride, TG], total lipid, free fatty acid, phospholipids [PhL], K^+, Ca^{2+}, and Fe^{3+}) were measured by the Kyoto Microorganism Institute (Kyoto, Japan).

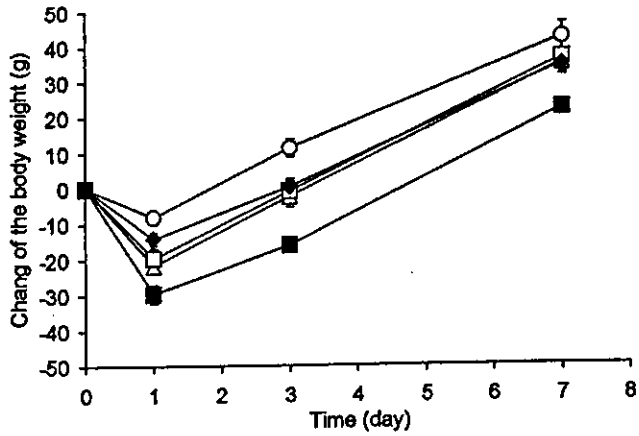

Figure 2. Body weight changes in male Wistar rats subjected to 20% and 40% blood exchange with recombinant human serum albumin (rHSA) and rHSA-heme solutions. Each value represents the mean±SEM. ○, Control group; ◆, 20% rHSA-heme group; △, 20% rHSA group; ■, 40% rHSA-heme group; and □, 40% rHSA group.

Histopathologic Observations

Paraffin sections were prepared from the 10% formalin fixed organs and stained with hematoxylin-eosin stain and Berlin blue. All histopathologic observations were carried out by Panapharm Laboratories Co., Ltd. (Kumamoto, Japan).

Data Analysis

The data for increased body weight, organ weight, and blood biochemical tests are expressed as mean ± SEM. A statistical analysis was performed using the Bartlett test followed by the Tukey-Kramer multiple comparison test. Values of $p < 0.05$ were considered significant. The statistical analytical software was StatView (SAS Institute Inc., Cary, NC).

Results

Appearance and Body Weight

In the control, 20% rHSA, and 20% and 40% rHSA-heme groups, all animals survived for 7 days without any change in their appearance and behavior. In contrast, one rat died after 3 days in the 40% rHSA group; the remaining five rats in this group did survive for 7 days.

In the control group, the change in body weight from the basal value decreased by 8.3 ± 1.5 gm after 1 day (**Figure 2**). However, it increased to 11.2 ± 2.4 gm after 3 days and to 42.1 ± 4.3 gm after 7 days.

In the 20% and 40% rHSA groups, body weights decreased by 21.8 ± 1.8 gm and 19.6 ± 2.8 gm, respectively, after 1 day, but they returned to basal levels after 3 days and increased to 34.9 ± 2.9 gm and 36.3 ± 4.0 gm, respectively, after 7 days.

In the 20% rHSA-heme group, body weight decreased by 14.3 ± 1.8 gm after 1 day. It recovered to the starting level after 3 days and increased to 34.9 ± 2.9 gm after 7 days. This change was almost the same as those observed in the 20% and 40% rHSA groups. In the 40% rHSA-heme group, the weight declined by 29.8 ± 2.5 gm after 1 day. Although it increased to 22.1 ± 2.1 gm after 7 days, the differences from the other groups were constant during the experimental period.

Weight of Vital Organs

We could not find any remarkable difference in the weights of the vital organs of the 20% rHSA and 20% rHSA-heme groups compared with the control group, except for spleen weight (**Figure 3**). Spleen weight was significantly increased in the 20% rHSA group after 1 and 7 days and in the 20% rHSA-heme group after 7 days.

In the 40% rHSA group, liver weight was significantly decreased after 1 day, and spleen weight increased after 7 days compared with that in the control group. In the 40% rHSA-heme group, spleen weight was significantly increased after 1 and 7 days *versus* the control group. There was no remarkable change in the weights of lungs, heart, liver, and kidney.

Blood Biochemical Tests

The 30 analytes from the blood biochemical tests of rat plasma are summarized in **Figure 4**. In the 20% and 40% rHSA groups, most of the parameters did not show any significant difference *versus* the control group, except for the iron decrease in the 20% rHSA group after 1 day and the choline esterase decrease after 7 days.

In the 20% rHSA-heme group, the decreases in LAP, TG, total lipid, PhL and iron after 1 day were significant compared with values in the control group. After 7 days, all analytes returned to the same levels as in the control group. With respect to the 20% rHSA group, the decrease in PhL after 1 day and the decrease in iron after 7 days were significant. In the 40% rHSA-heme group, the increase in total protein and AST and the decrease in total cholesterol, EChol, HDL cholesterol, and total lipid after 1 day were significant relative to the control group. Moreover, large increases in ALT and LDH were observed in three of the six samples. In comparison with the 40% rHSA group, the increase in LDH after 1 day, the decrease in EChol and HDL cholesterol after 1 day, the increase in HDL cholesterol after 7 days, and the decrease in TG after 7 days were significant.

Histopathologic Observations

A mild or modulate extramedullary hematopoiesis in the spleen was often found in all groups after the surgical operation at 7 days. In the 20% rHSA group, a slight erythrophagocytosis in the Kupffer cells of the liver (three samples) was observed after 7 days. In the 40% rHSA group, slight mineralization in the tubule of the kidney (three samples) after 1 day and a mild hyaline droplet in the tubule epithelial cells of the

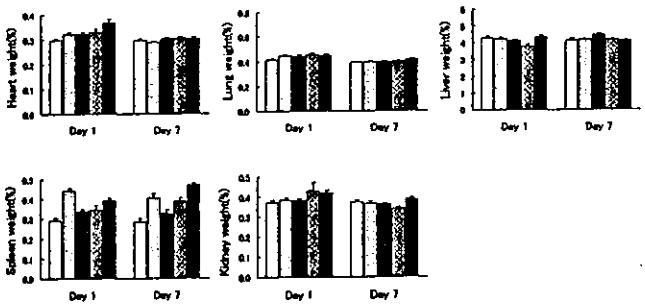

Figure 3. Relative organ weights (as a percentage of body weight) in male Wistar rats subjected to 20% and 40% blood exchange with recombinant human serum albumin (rHSA) and rHSA-heme solutions. Each value represents the mean±SEM. □, Control group; ▨, 20% rHSA group; ▩, 20% rHSA-heme group; ▨, 40% rHSA group; and ■, 40% rHSA-heme group.

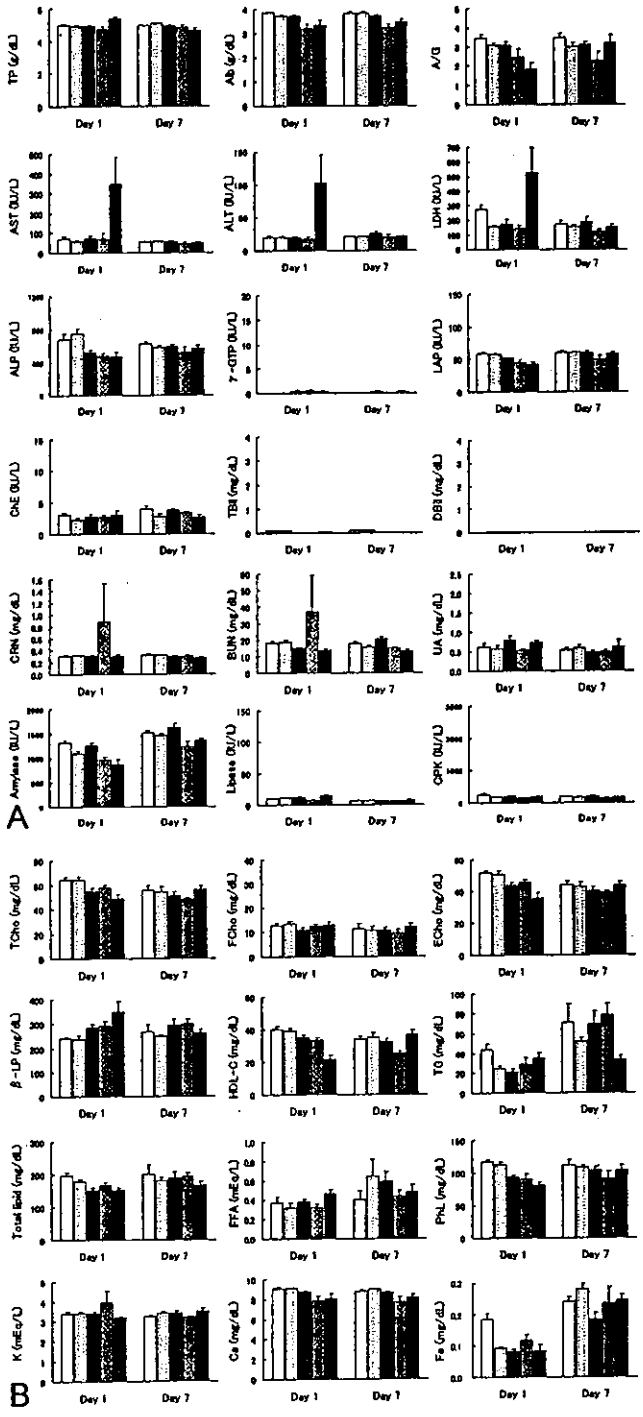

Figure 4. Blood biochemical tests of rat plasma after 20% and 40% blood exchange with recombinant human serum albumin (rHSA) and rHSA-heme solutions after 1 and 7 days. Each value represents the mean±SEM. □, Control group; ▨, 20% rHSA group; ▩, 20% rHSA-heme group; ▨, 40% rHSA group; and ■, 40% rHSA-heme group.

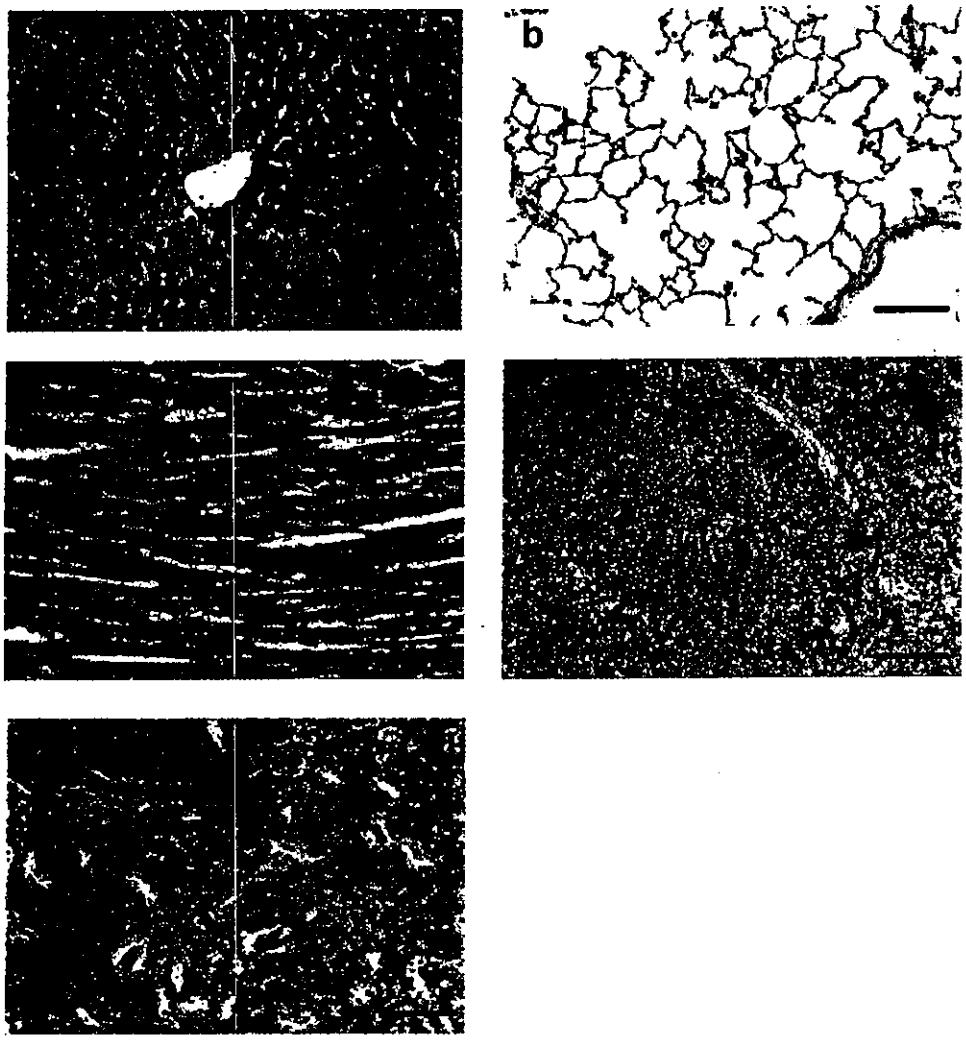

Figure 5. Microscopic observations of stained speciments of organs recovered from a rat 1 day after a 20% exchange with recombinant human serum albumin–heme. Bars = 100 mm, hematoxylin-eosin stain: a, liver; b, lung; c, heart; d, spleen; and e, kidney.

kidney (three samples) after 7 days were observed. There was no remarkable change in the lung, heart, and spleen.

In the 20% rHSA-heme group, a mild cellular infiltration in macrophages and a mild vacuolization in the Kupffer cells/macrophages of the liver were found in all six samples after 1 day (**Figure 5**). A mild brown pigment deposition appeared in the Kupffer cells/macrophages of the liver (five samples) after 7 days. There was no change in the heart, lung, and kidney. In the 40% rHSA-heme group, mild focal necrosis in the hepatocytes was visible in six samples after 1 day. The mild brown pigment deposition in the Kupffer cells/macrophages of the liver was also observed after 1 and 7 days. The mild hyaline droplet in the tubule epithelial cells in the kidney (three samples) was sometimes seen. There was no unusual change in the heart and lung.

Discussion

In the control group, although anesthesia and the surgical operation temporarily decreased the body weight of the animals after 1 day, it exceeded basal values after 3 days. The somewhat larger declines in body weight after the exchange transfusion with rHSA or rHSA-heme solution compared with the control group are considered to be the effect of hemodilution. To produce Hb, the iron concentration was reduced by consumption after 1 day. The decreased body weight increased at almost the same rate in all groups, and iron concentrations returned to control levels after 7 days.

The decrease in LAP, TG, total lipid, PhL, and iron in the 20% rHSA-heme group could not be related to acute toxicity. In addition, the mild cellular infiltration in macrophages and the mild vacuolization of Kupffer cells/macrophages in the liver observed after 1 day are considered to be a nonspecific biologic reaction to removal of the rHSA-heme, which was recognized to be an exogenous compound. More recently, we have found that >90% of the heme from the rHSA-heme is captured by the liver with high selectivity (Y. Huang *et al.*, unpublished data) After 7 days, a brown pigment deposit appeared in the Kupffer cells/macrophages of the liver. It gradually became fainter and finally disappeared after 2 months. If the heme is decomposed by hemeoxygenase in the same manner as protoheme IX from Hb, hemosiderin including free iron can be observed by Berlin blue staining. Contrary to our expectation, there was a very slight signal with the Berlin blue stain in the macrophages. We can conclude that the 20% blood exchange with the rHSA-heme solution did not produce any negative side effects in the rats.

We made further evaluations of the rHSA-heme solution with 40% blood replacement. In the 40% rHSA group, one rat died after 3 days. Although the reason is not clear, histopathologic data suggest occurrence of an unexpected disorder in the urinary system. No significant difference in the blood biochemical tests and organ weights of the 40% rHSA group in comparison with the control group (except for the decrease in liver weight after 1 day and an increase in spleen weight after 7 days) could be found. The increase in spleen weight was a specific biologic reaction to the administration of rHSA to the rats.

After a 40% blood exchange with the rHSA-heme solution, some liver function markers (*e.g.*, AST, ALT, and LDH) became elevated in three samples, and mild focal necrosis was observed in the liver after 1 day. Because these parameters in the 20% rHSA-heme group were similar or lower than those of the control group, this implies that some disorder in liver function might occur with a 40% blood exchange with the rHSA-heme solution. However, other liver function markers (γ-glutamyltransferase, total bilirubin, and direct bilirubin) remained unaltered after sample infusion, so the "disorder" seems to have been temporary and not serious. Similar to the 20% rHSA-heme group after 7 days, the brown pigment deposit in the Kupffer cells/macrophages, which is presumably heme itself or a decomposition thereof, was also found. The results of the blood biochemical tests and the histopathologic observations returned to normal after 7 days.

In conclusion, the 20 % blood replacement with rHSA-heme in rats did not yield any toxic side effects for 7 days. A mild liver disorder occurred in the 40% rHSA-heme group; however, liver function returned normal within 7 days. Thus, administration of the rHSA-heme solution in a volume of 20% total blood volume did not produce any dysfunction of the vital organs, which allows us to undertake further advanced preclinical testing of this synthetic O_2 carrier as a red blood cell substitute.

Acknowledgment

The authors are grateful to NIPRO Corp. for their supporting the O_2 infusion project.

References

1. Tsuchida E: Perspectives of blood substitutes, in Tsuchida E (ed), *Blood Substitutes: Present and Future Perspectives,* Lausanne: Elsevier Science, 1998, pp. 1–14.
2. Winslow RM: The role of blood substitutes in emerging healthcare systems, in Tsuchida E (ed), *Blood Substitutes: Present and Future Perspectives,* Lausanne: Elsevier Science, 1998, pp. 15–32.
3. Squires JE: Artificial blood. *Science* 295: 1002–1005, 2002.
4. Greenburg AG, Kim HM: Hemoglobin-based oxygen carriers. *Crit Care* 8: S61–64, 2004 (and references therein).
5. Vandegriff KD, Malavalli A, Wooldridge J, Lohman J, Winslow RM: MP4, a new nonvasoactive PEG-Hb conjugate. *Transfusion* 43: 509–516, 2003.
6. Simoni J, Simoni G, Wesson DE, Griswold JA, Feola M; A novel hemoglobin-adenosine-glutathione based blood substitute: Evaluation of its effect on human blood *ex vivo. ASAIO J* 46: 679–692, 2000.
7. Powanda DD, Chang TMS: Cross-linked polyhemoglobin-superoxide dismutase-catalase supplies oxygen without causing blood-brain barrier disruption or brain edema in a rat model of transient global brain ischemia-reperfusion. *Artif Cells Blood Subs Immobil Biotechnol* 30: 23–27, 2002.
8. Komatsu T, Hamamatsu K, Wu J, Tsuchida E: Physicochemical properties and O_2-coordination structure of human serum albumin incorporating tetrakis(*o*- pivamido)phenylporphyrinatoiron(II) derivatives. *Bioconj Chem* 10: 82–86, 1999.
9. Tsuchida E, Komatsu T, Matsukawa Y, Hamamatsu K, Wu J: Human serum albumin incorporating tetrakis(o-pivalamido)-phenylporphinatoiron(II) derivative as a totally synthetic O_2-carrying hemoprotein. *Bioconj Chem* 10: 797–802, 1999.
10. Komatsu T, Matsukawa Y, Tsuchida E: Effect of heme structure on O_2-binding properties of human serum albumin–heme hybrids: Intramolecular histidine coordination provides a stable O_2-adduct complex. *Bioconj Chem* 13: 397–402, 2002.
11. Tsuchida E, Komatsu T, Hamamatsu K, *et al:* Exchange transfusion of albumin-heme as an artificial O_2-infusion into anesthetized rats: Physiological responses, O_2 delivery and reduction of the oxidized hemin sites by red blood cells. *Bioconj Chem* 11: 46–50, 2000.
12. Huang Y, Komatsu T, Nakagawa A, Tsuchida E, Kobayashi S: Compatibility *in vitro* of albumin-heme (O_2 carrier) with blood cell components. *J Biomed Mater Res* 66A: 292–297, 2003.
13. Tsuchida E, Komatsu T, Matsukawa Y, *et al:* Human serum albumin incorporating synthetic heme: Red blood cell substitute without hypertension by nitric oxide scavenging. *J Biomed Mater Res* 64A: 257–261, 2003.
14. Komatsu T, Yamamoto H, Huang Y, Horinouchi H, Kobayashi K, Tsuchida E: Exchange transfusion with synthetic oxygen-carrying plasma protein 'albumin-heme' in acute anemia rat model after seventy-percent hemodilution. *J Biomed Mater Res* 71A: 2004, in press.
15. Huang Y, Komatsu T, Yamamoto H, Horinouchi H, Kobayashi K, Tsuchida E: Exchange transfusion with entirely synthetic red-cell substitute albumin-heme into rats: physiological responses and blood biochemical tests. *J Biomed Mater Res* 71A: 63–69, 2004.

Human Serum Albumin Bearing Covalently Attached Iron(II) Porphyrins as O_2-Coordination Sites

Rong-Min Wang,[†,‡] Teruyuki Komatsu,[†] Akito Nakagawa,[†] and Eishun Tsuchida*[,†]

Advanced Research Institute for Science and Engineering, Waseda University, 3-4-1 Okubo, Shinjuku-ku, Tokyo 169-8555, Japan, and Institute of Polymer, Northwest Normal University, Lanzhou 730070, China . Received June 17, 2004; Revised Manuscript Received September 25, 2004

Tetrakis{(α,α,α,α-*o*-pivalamido)phenyl}porphinatoiron(II) with a bifunctional tail possessing an axially coordinated imidazolyl group and a protein attachable succinimidyl(glutamyl) group (FeP-GluSu) has been synthesized. It can efficiently react with the lysine residues of recombinant human serum albumin (rHSA), giving a new albumin–heme conjugate [rHSA(FeP-Glu)]. MALDI-TOFMS showed a distinct molecular ion peak at *m/z* 70 643, which indicates that three FeP-Glu molecules were covalently linked to the rHSA scaffold. The binding number of FeP-Glu is approximately three (mol/mol) and independent of the mixing ratio. The CD spectrum and Native PAGE revealed that the albumin structure remained unaltered after the covalent bonding of the hemes. This rHSA(FeP-Glu) conjugate can bind and release O_2 reversibly under physiological conditions (pH 7.3, 37 °C) in the same manner as hemoglobin and myoglobin. The O_2-adduct complex had a remarkably long lifetime ($\tau_{1/2}$: 5 h). The O_2-binding affinity [$P_{1/2}^{O_2}$: 27 Torr] was identical to that of human red cells. Laser flash photolysis experiments gave the O_2- and CO-association rate constants and suggested that there are two different geometries of the imidazole binding to the central ion.

Human serum albumin (HSA), which is the major plasma protein component in our bloodstream, has no prosthetic group; however it nonspecifically captures many endogenous and exogenous compounds by weak interactions, *e.g.*, H-bond, ionic attraction, and hydrophobic interaction, namely noncovalent bonds (*1–3*). Synthetic heme, 2-[{8-*N*-(2-methylimidazolyl)octanoyl}-oxy]methyl-5,10,15,20-tetrakis{(α,α,α,α-*o*-pivalamido)-phenyl}porphinatoiron(II) (FeP, Chart 1 a) is also incorporated into recombinant HSA (rHSA), and the obtained albumin–heme (rHSA-FeP) hybrid can reversibly coordinate O_2 under physiological conditions (pH 7.3, 37 °C) (*4*). This O_2-carrying plasma hemoprotein could be of medical importance as a blood replacement composition (*4e–g*). Nevertheless, the major driving force of the heme-binding to albumin is a hydrophobic interaction; therefore, its binding constants (10^4–10^6 M^{-1}) are not high enough to maintain the heme concentration in the circulatory system for a long period (*4a*). The administration of the albumin–heme hybrid solution into rats demonstrated that the lifetimes of the heme was less than 6 h (*4e, 5*). To immobilize the heme group to the albumin scaffold more tightly and retain its O_2-transport efficacy, we have combined the O_2-coordination site FeP to the rHSA structure through a covalent bond. In this communication, we report, for the first time, the synthesis of a novel FeP analogue with a bifunctional branched-tail including an axially coordinated imidazolyl group and a protein-attachable succinimidyl(glutamyl) group (FeP-GluSu, Chart 1 a), and the properties of the rHSA conjugate bearing covalently linked FeP-Glu as a new O_2-carrying hemoprotein.

Chart 1. (a) 5,10,15,20-Tetrakis{(α,α,α,α-*o*-pivalamido)-phenyl}porphinatoiron Derivatives with a Bifunctional Tail Group. (b) Space-Filling Representation of the Oxygenated FeP-GluSu by Insight II (see ref 11)

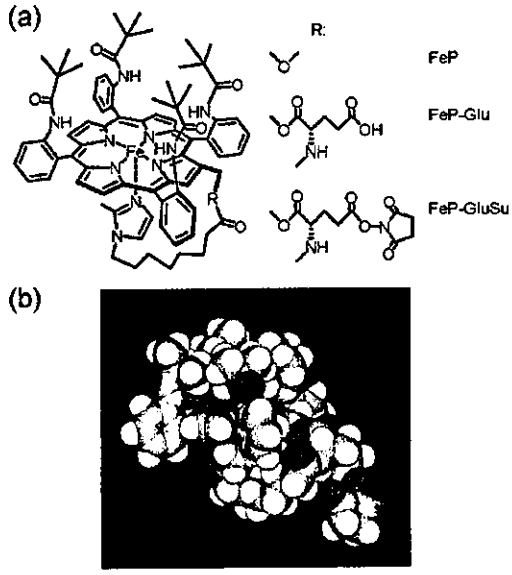

As a functional side-chain of FeP, which directly makes a covalent bond to rHSA, we selected the succinimidyl group, because it selectively reacts with the NH_2 group of lysine in the range of pH 6.3–8.6 with high yield. The branched tail that includes the imidazolyl and succnimidyl groups via a glutamate junction was introduced into the parent porphyrin 1 (*6*) as shown in Scheme 1 (*7*).

* Corresponding author. Phone: +81 3-5286-3120. Fax: +81-3-3205-4740. E-mail: eishun@waseda.jp.
† Waseda University.
‡ Northwest Normal University.

10.1021/bc049859m CCC: $30.25
Published on Web 11/12/2004

Scheme 1. Synthetic Scheme of FeP-GluSu

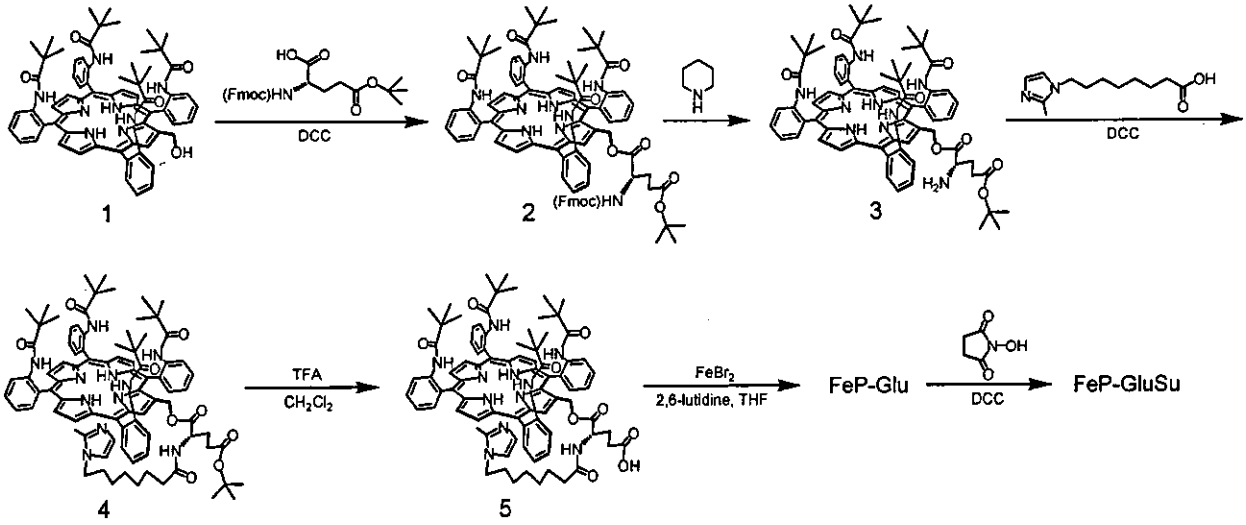

Table 1. CO-and O_2-Binding Parameters of rHSA(FeP-Glu) Conjugate in Phosphate–Buffered Solution (pH 7.3) at 25 °C

	$10^{-6}\,k_{on}^{CO}(M^{-1}s^{-1})$		$10^{-7}\,k_{on}^{O_2}(M^{-1}s^{-1})$		$10^{-2}\,k_{off}^{O_2}(s^{-1})$		$P_{1/2}^{O_2}$(Torr)[a]
system	fast	slow	fast	slow	fast	slow	
rHSA(FeP-Glu) conjugate	6.2	1.1	2.8	–	3.3	–	9 (27)
rHSA-FeP hybrid[b]	4.7	0.66	3.2	1.0	7.2	2.2	13 (35)
Hb(T-state)α[c]	0.22	–	0.29	–	1.8	–	40

[a] At 37 °C in parenthesis. [b] From ref 4c. [c] From refs 13–15.

First, Fmoc-L-Glu(g-*tert*-butyl ester) was bound to the OH group at the β-pyrrolic position of the porphyrin **1** by DCC. After removal of the Fmoc protecting group with piperidine, 8-*N*-(2-methylimidazolyl)octanoic acid was reacted with the obtained compound **3** in CH_2Cl_2, giving the imidazolyl-tailed porphyrin (**4**). The *tert*-butyl group was then removed by TFA, and the central iron insertion was carried out by the general $FeBr_2$ method to afford the iron-porphryin FeP-Glu. Finally, the reaction of *N*-hydroxysuccinimide with DCC gave the FeP-GluSu. All reactions can be performed at room temperature with high yields. The analytical data of all compounds described above were satisfactory obtained (*7*).

The FeP-Glu was converted to the ferrous complex by reduction in a heterogeneous two-phase system (toluene/aqueous $Na_2S_2O_4$) under an N_2 atmosphere (*6, 8*). The UV–vis absorption spectrum of the orange solution showed five-*N*-coordinated Fe(II) species (λ_{max}: 440, 531, 563 nm) via intramolecular imidazole binding (*6, 8, 9*). Upon exposure to CO, its UV–vis absorption immediately moved to that of the CO adduct complex. On the other hand, the dioxygenation was unstable at 25 °C, which is likely due to the presence of the neighboring glutamic acid proton.

The EtOH solution of the carbonyl FeP-GluSu (2 mL) was then injected into the phosphate-buffered solution of rHSA (8 mL, pH 7.3) (molar ratio 4/1), and the mixture was gently stirred for 1 h at room temperature. The solution was dialyzed against phosphate buffer (pH 7.3) to remove EtOH. The MALDI-TOFMS demonstrated a single molecular ion peak at *m/z* 70 643 (Figure 1). Attempts to measure the molecular weight of the rHSA-FeP hybrid, in which the FePs are noncovalently accommodated, failed using MALDI- and ESI-TOFMS; the molecular ion peak of rHSA (65 500) was only observable because the FePs are dissociated from the albumin during the ionization process (*10*). Therefore, we can conclude that the FeP-Glu is conjugated with rHSA through amide bond formation. The average number of FeP-Glu in an rHSA was estimated to be 2.9–3.5, and this number is not dependent on the mixing molar ratio of FeP-GluSu/rHSA that ranged from 4 to 10. There are a total of 59 NH_2 groups in the rHSA structure, but only three of them are presumably active for the FeP-GluSu binding.

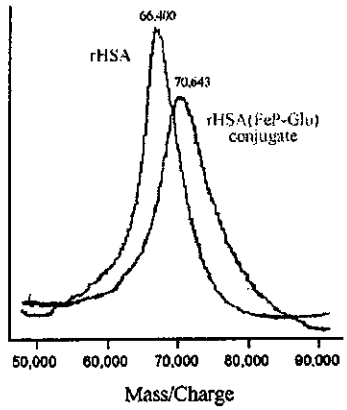

Figure 1. MALDI-TOFMS of the rHSA(FeP-Glu) conjugate. Matrix: 2,5-dihydroxybenzoic acid.

The conjugation of FeP-GluSu did not induce any change in the circular dichroism spectrum of rHSA in the 200–250 nm region. The Native PAGE of rHSA(FeP-Glu) also showed a single band with same migration distance of rHSA. Both results suggested that the secondary structure, molecular shape, and surface charge of albumin remained unaltered after the covalent binding of the hemes.

The UV–vis absorption spectrum of the rHSA(FeP-Glu) conjugate under an N_2 atmosphere showed a typical five-*N*-coordinated complex as seen in the toluene solution of FeP-Glu (Figure 2) (*4a,b, 6, 8, 9*). Upon exposure

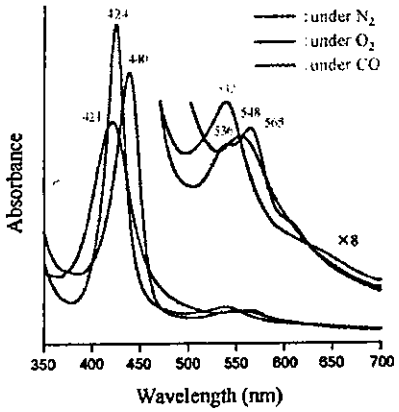

Figure 2. UV–vis absorption spectral changes of the rHSA-(FeP-Glu) conjugate in phosphate-buffered solution (pH 7.3) at 25 °C.

of this solution to O_2, the spectrum changed to that of the O_2-adduct complex under physiological conditions (pH 7.3, 37 °C) (*4a–c*). This dioxygenation was reversibly observed to be dependent on the O_2 partial pressure in the same manner as hemoglobin (Hb) and myoglobin. The half-lifetime of the O_2 adduct (ca. 5 h at 37 °C) was significantly longer than that of the noncovalent rHSA-FeP hybrid ($\tau_{1/2}$: 2 h) (*4d*). The covalent linkages of FeP-Glu to the protein scaffold obviously retarded the oxidation process of the central ferrous ion. Molecular simulation of the structure of FeP-GluSu revealed that the geometry of the imidazole ring against the porphyrin platform was perpendicular, which suggests that the spacer moiety between the imidazole and the porphyrin periphery does not produce an unfavorable distortion of the axial coordination and will not influence the O_2-binding behavior (see Chart 1b) (*11*).

The O_2-binding affinity [$P_{1/2}{}^{O_2}$] of the rHSA(FeP-Glu) conjugate was determined to be 27 Torr at 37 °C (*3b,c, 6, 7, 9, 10*), which is almost the same as that of the rHSA-FeP hybrid [$P_{1/2}{}^{O_2}$: 33 Torr] (*3b–d*) and identical to that of human red cells (*12*). The laser flash photolysis experiments provided the association rate constants of the O_2- and CO-bindings ($k_{on}{}^{O_2}$, $k_{on}{}^{CO}$) (*6, 8, 9a*). The absorption decays accompanying the O_2- and CO-recombination to the noncovalent rHSA-FeP hybrid were composed of two phases of the first-order kinetics, and the curves were fit by a double-exponential equation to determine k_{on} (fast) and k_{on} (slow) (Table 1) (*4c*). We supposed that the O_2- and CO-association to the FeP in the hydrophobic domains of the albumin was influenced by the molecular microenvironments around each O_2-coordination site, e.g., steric hindrance of the amino acid residue and difference in polarity (*4b–d*). The time dependence of the absorption change in the CO recombination to the rHSA(FeP-Glu) conjugate also showed double-exponential profile, but the rebinding process of O_2 obeyed monophasic decay. On the basis of studies on synthetic model hemes, it has been known that the proximal-side effect is the only primary factor which influences the association rate for CO but not for O_2 (*8, 9a*). We assume that there are two different geometries of the imidazole coordination and that each one shows the individual kinetics of the CO association. The covalent linkages between the axially coordinated imidazolyl side-chain and the albumin structure may provide an additional strain of the Fe–N(imidazole) bond and gives two conformations of the proximal-base binding. Since the $k_{on}{}^{O_2}$ value of rHSA(FeP-Glu) was nearly the same as the $k_{on}{}^{O_2}$ (fast) of the rHSA-FeP hybrid (Table 1), the FeP-Glu molecules are likely to locate on the surface of rHSA.

In conclusion, reaction of the newly synthesized tetrakis{(α,α,α,α-*o*-pivalamido)phenyl}porphinatoiron(II) with a proximal base and succinimidyl(glutamyl) group to rHSA produced a novel albumin conjugate bearing covalently attached heme groups as O_2-coordination sites. The molecular weight of rHSA(FeP-Glu) was directly measured by MALDI-TOF MS. In nature, one can find unique heme-linked proteins, e.g., cyctochrome *c*. The rHSA(FeP-Glu) conjugate presumably becomes a valuable model of these hemoproteins. The obtained rHSA-(FeP-Glu) can reversibly absorb O_2 under physiological conditions, and its O_2-binding affinity showed an identical value to that for human erythrocytes. These results suggest that this novel plasma protein may efficiently transport O_2 in the bloodstream as an O_2-carrier with a long circulation time.

ACKNOWLEDGMENT

This work was partially supported by Grant-in-Aid for Scientific Research (No. 16350093) from JSPS, Grant-in-Aid for Exploratory Research (No. 16655049) from MEXT Japan, and Health Science Research Grants (Regulatory Science) from MHLW Japan. R.M.W. acknowledges NNSFC (No. 20274034). The authors are grateful to NIPRO Corp. for their supporting the oxygen-infusion project.

Supporting Information Available: Experimental details of the compounds **2**, **3**, **4**, **5**, FeP-Glu, and FeP-GluSu and their spectroscopic data. This material is available free of charge via the Internet at http://pubs.acs.org.

LITERATURE CITED

(1) Peters, T., Jr. (1996) All about albumin. *Biochemistry, Genetics, and Medical Applications*, Academic Press, San Diego; and reference therein.
(2) Kragh-Hansen, U. (1981) Molecular aspects of ligand binding to serum albumin. *Pharmacol. Rev. 33*, 17–53.
(3) Curry, S., Brick, P., and Franks, N. P. (1999) Fatty acid binding to human serum albumin: new insights from crystallographic studies. *Biochim. Biphys. Acta 1441*, 131–140.
(4) (a) Komatsu, T., Hamamatsu, K., Wu, J., and Tsuchida, E. (1999) Physicochemical properties and O_2-coordination structure of human serum albumin incorporating tetrakis(*o*-pivamido)phenylporphyrinatoiron(II) Derivatives. *Bioconjugate Chem. 10*, 82–86. (b) Tsuchida, E., Komatsu, T., Matsukawa, Y., Hamamatsu, K., and Wu, J. (1999) Human serum albumin incorporating tetrakis(*o*-pivalamido)phenylporphinatoiron(II) derivative as a totally synthetic O_2-carrying hemoprotein. *Bioconjugate Chem. 10*, 797–802. (c) Komatsu, T., Matsukawa, Y., and Tsuchida, E. (2000) Kinetics of CO- and O_2-binding to human serum albumin-heme hybrid. *Bioconjugate Chem. 11*, 772–776. (d) Komatsu, T., Matsukawa, Y., and Tsuchida, E. (2002) Effect of heme structure on O_2-binding properties of human serum albumin-heme hybrids: intramolecular histidine coordination provides a stable O_2-adduct complex. *Bioconjugate Chem. 13*, 397–402. (e) Tsuchida, E., Komatsu, T., Hamamatsu, K., Matsukawa, Y., Tajima, A., Yoshizu, A., Izumi, Y., and Kobayashi, K. (2000) Exchange transfusion of albumin-heme as an artificial O_2-infusion into anesthetized rats: physiological responses, O_2-delivery and reduction of the oxidized hemin sites by red blood cells. *Bioconjugate Chem. 11*, 46–50. (f) Kobayashi, K., Komatsu, T., Iwamaru, A., Matsukawa, Y., Watanabe, M., Horinouchi, H., and Tsuchida, E. (2003) Oxygenation of hypoxia region in solid tumor by administration of human serum albumin incorporating synthetic hemes. *J. Biomed. Mater. Res. 64A*, 48–51. (g) Tsuchida, E., Komatsu, T., Matsukawa, Y., Nakagawa, A., Sakai, H., Kobayashi, K., and Suematsu, M. (2003) Human serum albumin incorporating synthetic heme: red blood cell substitute